ADVANCED INTELLIGENT SYSTEMS
Open Access
www.advintellsyst.com

Bioinspired Morphing Mechanisms for Soft Systems: A Review

*Oscar Rabaux and Christine Jérôme**

Throughout evolution, plants have developed a number of strategies to induce movement ensuring the survival and reproduction of their species. Carnivorous plants feed by trapping insects, sunflowers grow by following the sun, and pine cones control the dispersal of their seeds under optimal conditions. This comprehensive review first analyses the mechanisms responsible for these adaptive movements highlighting the need for a gradient in one of the physico-chemical properties to enable morphing. Next, the main synthetic shape-changing soft systems are presented in terms of their mechanism of action. A gradient in water-swelling, magneto-rheological properties, residual deformation, or extensibility gives hygromorphs, magnetomorphs, mechanomorphs, and baromorphs, respectively. The various morphing triggers, namely light, heat, pH, tensile stress, pressure, electric, and magnetic fields, are described. The opportunities and challenges of each system are put into perspective. This report aims to provide the reader with a toolbox for designing shape-changing materials considering the targeted trigger, as well as providing a deeper understanding of the underlying mechanisms paving the way for future discoveries.

1. Introduction

Morphing is the specific behavior of a living (plants, fungi) or a synthetic system which changes its shape upon a trigger. Inspired by nature, it has been extensively studied for industrial needs because it is a science that facilitates the production of complex 3D shapes from flat sheets whose shape adaptation can be delayed. Most of the time, the living or manufactured object responds remotely to external stimuli such as humidity, solvent, pH, temperature, light, voltage, and magnetic field. Some actuations require a contact when the stimulus is a (uniaxial) load, pressure, or electric current This capacity is the result of a gradient in one of the thermo-chemo-mechanical property either in- plane or out-of-plane, responsible for differential eigenstrains.[1] It was first studied and theorized on metals almost 100 years ago, notably by Stephen Timoshenko, father of a model for bimetallic thermostats that is still used to predict the shape change of a bilayer material.[2] Slight modifications have sometimes been needed for specific modeling, for instance for the ZnO piezoelectric actuator of Pisano which was at the limit of one of the assumptions, namely that the thickness of the bonding layer is no longer negligible in the case of thin layers.[3] More recently, these principles have been applied to complex ceramic parts or to ease the fabrication of tiles on roofs with modest raw materials.[4,5] Obtaining complex shapes in ceramic parts has always been a challenge and, until now, the processes involved locally weak joints that weakened the parts as a whole. Studart et al. proposed to align magnetized alumina platelets with a rotating magnetic field differentially in two layers, resulting in differential shrinkage during sintering and allowing highly curved or twisted objects to be obtained. This self-folding principle can also be used in daily-life applications to build tiles from local raw materials, such as celery fibers, clay, and starch which take shape as they dry and could make a real contribution to improving modest housing throughout the world. However, metals and ceramics are very stiff materials that cannot undergo large deformations which severely limits their use in this type of applications. An alternative for these stiff materials is to induce deformations using folds cut according to the model inspired by kirigami and miura-ori folding.[6] In the 1930s, the discovery of synthetic macromolecules that were 10–1000 times more flexible, stretchable, and above all multiresponsive made these organic materials the major components of the systems studied in the field of morphing.

Inspired by nature and the numerous shape-adaptation mechanisms of plants for seed dispersal, efficient growth, and feeding, the synthetic systems nowadays display various possibilities for state-of-the-art applications. Recent generalist reviews in 2020 interestingly list the shaping actuators by class of materials including the shape-memory polymers or by actuation triggers.[7,8] Herein, we aim reviewing the shape-changing materials rather than focusing on mechanisms to give the readers updated keys on how morphing can be obtained and actuated. Shape-memory polymers whose shape change requires programming, fixing, and recovery have been deliberately excluded from the scope of this review.

O. Rabaux, C. Jérôme
Center for Education and Research on Macromolecules
University of Liège
4000 Liège, Belgium
E-mail: c.jerome@uliege.be

The ORCID identification number(s) for the author(s) of this article can be found under https://doi.org/10.1002/aisy.202400331.

DOI: 10.1002/aisy.202400331

In this review, we aim to show that most of the morphing mechanisms involved in synthetic systems have already been used in nature and are therefore very often bioinspired (**Figure 1**). Thus, it starts with an overview of the morphing mechanisms developed by plants for survival and reproduction. The synthetic systems will then be linked to one of these mechanisms, providing a better understanding of the principle of remote triggering. The most emblematic adapting plants, i.e., the pinecone and the *Dionaea muscipula* or Venus flytrap, which have led to bioinspired *hygromorphs* (differential swelling) with several possible actuations depending on the nature of the hydrogel, will be discussed first.[9] Next, we propose to name *magnetomorphs* systems in which embedded magnetic particles deform a soft material. Then come *mechanomorphs*, which adapt their shapes according to a differential recovery of strains, and are actuated by different triggers depending on the nature of the materials and the *baromorphs* which are specific systems in which air-channels in soft materials can be pressurized. As the names "hygromorph" and "baromorph" are already in common use, similar terms have been applied to the other families to facilitate comparisons. Finally, we will review the most recent advances in other kinds of mechanisms such as cell contraction. The remaining main challenges will be highlighted. One of the most important dilemmas is clearly the size upscaling of these systems, the autonomous response to external triggers, and the reduction in energy consumption. For instance, for applications to new weather-adaptive houses,[10] the major aspect is also the time of response, and here again plants can give us examples of how to speed up the movements with the multistable carnivorous plants. This is also the subject of a review from 2022.[11] Reviewing this field by mechanisms will, we hope, enable new breakthroughs to be made thanks to an overview and comprehensive understanding of the concepts underlying shape change. Finally, our objective is also to highlight the materials currently available for such morphing systems that are compatible with applications in the healthcare field.

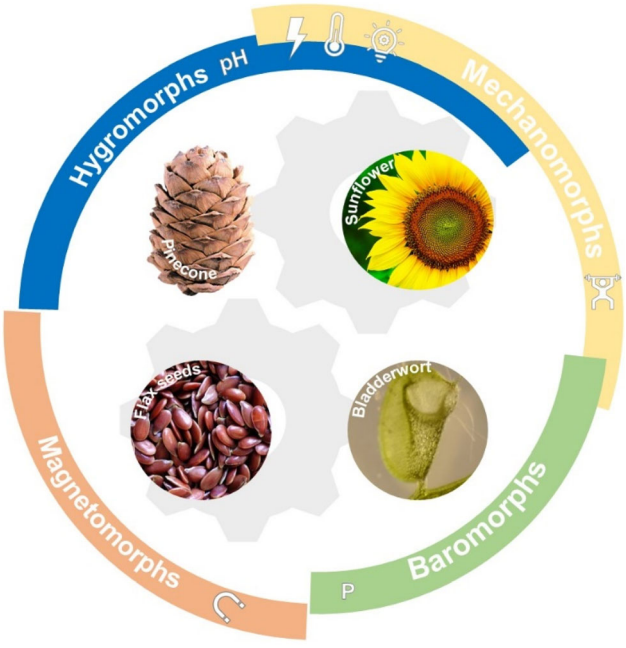

Figure 1. General scheme of bio-inspired morphing materials and their triggers.

2. Morphing in Nature

2.1. Differential Swelling

Several plants use differential swelling to actuate morphing and disperse seeds efficiently.[12] Others use it for feeding. Among these, the pinecone and the *Dionaea muscipula* or Venus flytrap are certainly the most representative and well-known examples. The first one is used as a humidity sensor in the daily life of numerous people, while the second one participates in the legend of carnivorous plants. While in the pinecone, morphing is a passive phenomenon, it is active in the flytrap. Other examples of passive plants using differential swelling are also presented and compared with the pinecone to deduce shape adaptability strategies.

The pinecone self-opens to release its seeds only by dry weather for more efficient seed-dispersion. To this end, each of the pine cone's ovuliferous scales, between which the seeds are located, is a bilayer material made up of a passive layer, which does not absorb moisture, and an active layer, which absorbs moisture (**Figure 2**A). The passive upper layer consists of sclerenchyma fibers, long fibers parallel to the direction of the scale made of cellulose, pectin, and lignin. The active layer underneath consists of more hydrophilic sclerids, short fibers perpendicular to the direction of the scale, containing significantly less lignin which is hydrophobic.[13] The folding comes from both the differential directions and the different nature of the fibers, where sclerids are more hydrophilic than sclerenchyma. The movement is amplified by a second type of scale named bract (Figure 2A), which is beneath each ovuliferous scale. It is a thicker but smaller and swelling scale that remains close to the pinecone body.[14] Here, the scale movement is restricted by the next scale and the stiff body, then the bending is relatively low and slow with a maximum angle difference between wet and dried states of 90° within 100 min.[15] Perhaps the most interesting feature of the pinecone is that this folding mechanism is still working when the pinecone is no longer on the tree making it a practical and costless passive system for detecting humidity in our environment. Moreover, it is perfectly reversible upon moisture changes.

Creating bilayers with materials of different hydrophilicity and thus water swelling is at the basis of efficient and long-term reversible folding in response to humidity variation.

Wheat awns use morphing to bury seeds in the ground by a back and forth lever movement of two long stems attached to the seed. Similar to pinecone, the shape change comes from a differential humidity uptake between one active (ridge) and one passive layer (cap) (Figure 2B).[16] It is more sensitive to humidity than the pinecone allowing bending on one side to dry air during the day and on the other in damp air at night. In contrast to pinecones, the chemical nature of the layers is similar with only the orientation of cellulose fibrils differing: parallel in the cap, random in the ridge. The reason of the increased sensitivity is that the alignment of the cellulose fibrils in the cap induces longer

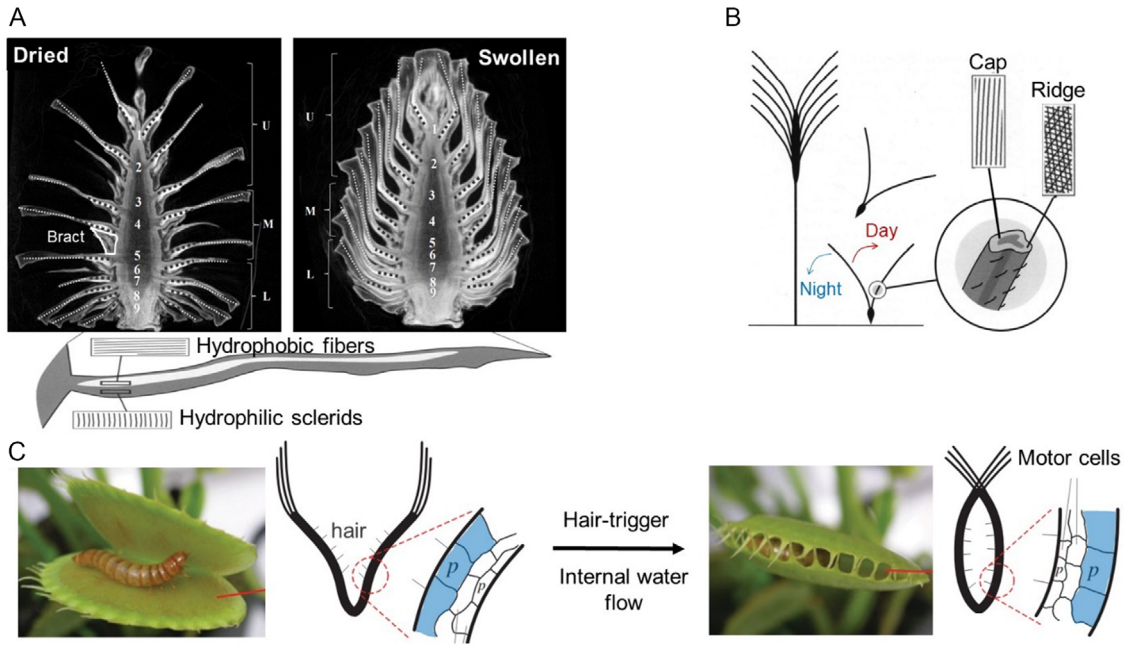

Figure 2. A) Pinecone morphological structure [Reproduced under the terms of the CC-BY 4.0 license.[14,16]], B) wheat awn burying seed [Reproduced with permission.[16] Copyright 2024, RSC], C) Venus flytrap internal water flow [Reproduced with permission.[6] Copyright 2024, RSC].

crystalline domains enhancing the difference of swelling ability even though the water uptake by the amorphous matrix is similar in both layers.[17] Interestingly, the ridge dries faster than the cap, as the fibrils are not random at the nanoscale, but form a succession of rings with alternating parallel and perpendicular fibrils, resulting in internal buckling during drying and accelerating vapor diffusion out of the material.

Bauhinia variegate is another example of a plant that folds as a result of the differential swelling of two chemically identical layers that fibers are oriented differently. Here the directions are $+45°$ and $-45°$ with respect to the long axis, which induces torsion instead of uniaxial bending according to the classic theory of laminates.[18,19]

Controlling the orientation of crystallization is a second way of accelerating the folding response in bioinspired materials.

The *Aizoaceae* or ice plant uses morphing also for seed dispersal but here opens up in wet conditions to assist the seed with proper germination conditions.[20] It opens by 180° in a few minutes due to structured hexagonal cells amplifying the difference between the dried and wet states. This plant is not a bilayer, but the swelling is anisotropic in these hexagonal cells with around four times more extension in one direction compared to the perpendicular direction, resulting in the opening. It is a typical example of in-plane gradient of the swelling capacity.

To catch flying preys to feed themselves, one family of carnivorous plants had to find a way to speed up its response to flies landing, in the millisecond range instead of the hundreds of minutes. This was achieved by the *Dionaea muscipula* which responds directly via its lobes and by the *Aldrovanda vesiculosa* which responds via a central midrib guiding the passive lobes.[21] Here again, folding is induced by a bilayer system, but instead of having differential absorption, the water entrapped in the plant tissues goes from one layer to the other upon mechanical trigger of the external hair inducing an electrical response to open pores between both layers (Figure 2C).[22] The reason for the extraordinary fast response (100 ms) lies in the metastable position of the lobes or midrib at rest.[23] The shape switch is obtained even after an incomplete transfer of water between the layers because after a small perturbation the plant will snap toward a lower energy position (closed state). Interestingly for the transposition of this mechanism to synthetic systems, the snapping can also be activated by an electric current between one lobe and the midrib bypassing the plant hairs.[22]

Folding in response to a local trigger, in this case, the fly landing on the plant hairs, can be accelerated via metastable shapes.

2.2. Differential Growth

Cyclamen hederifolium and *Helianthus annuus* or sunflower are two plants using differential growth between two sides of their stems to bend. For the cyclamen, it is inherent to the plant to protect the seed and guarantee germination, while for the sunflower, it is activated by the sun direction, a so called heliotropic movement. In both stems, there is a local heterogeneity in the distribution of the auxin growth hormone. Due to this local increase of auxin, one side of the cyclamen grows faster at 60–200 $\mu m\,h^{-1}$, and the stem is fully coiled on itself within a week (**Figure 3**A).[24] For the sunflower, there is always more auxin on the shaded side of the stem causing to bend reversibly by following the sun during the day. Two hypotheses are up to now discussed, either an auxin redistribution within the stem to always be in the shaded side or a favored auxin production on the shaded side.[25,26] This has been proved to be heliotropic, meaning that the movement depends on the direction of the trigger.

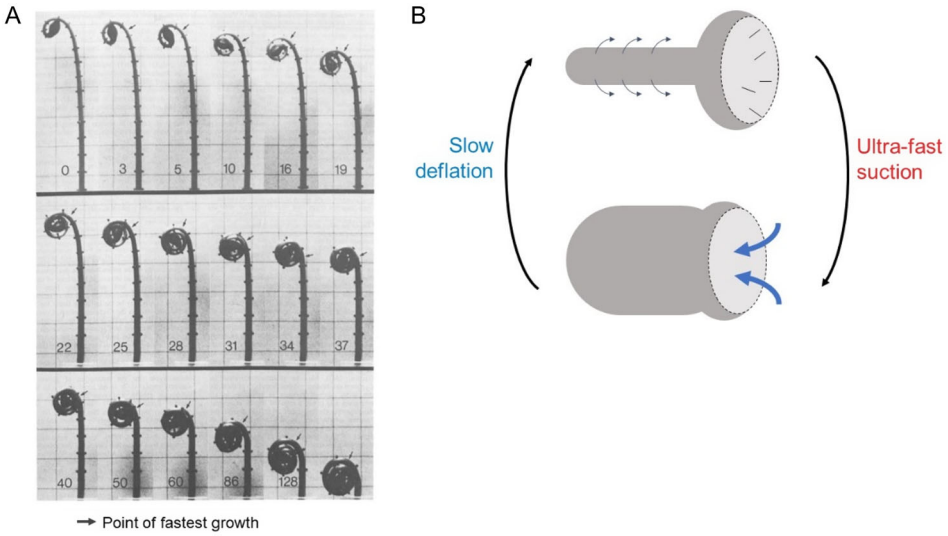

Figure 3. A) Self-rolling cyclamen [Reproduced with permission.[24] Copyright 2024, Wiley], B) scheme of prey-catching bladderworts.

Indeed, when the sunflowers are grown with an artificial light overhead they are not bending at all.[26] However, because this morphing behavior is mediated by the growth of the plant, it is irreversible. Indeed, after flower maturation, the sunflower faces east all day long without moving anymore, which is an intrinsic evolution strategy to attract pollinators.[27]

Differential growth can also be activated externally even though the natural system does not bend in classical growth conditions. Indeed, *Phycomyces* a species of fungus grows in the dark but growth can be stimulated by light. When the incident light is perpendicular to the growing stem which is constituted of an inner photo-responsive wall and an outer passive wall, the fungus can bend.[28] Interestingly, it is much more rapid than the cyclamen with a local growth which can go up to 4 mm h^{-1} and a bending of 5°–7° min^{-1}. Instead of light activation, growth can also be enhanced by external magnetic fields, as it was evidenced when studying the influence of the geomagnetic field on the most consumed cereals.[29] For instance, barley and oat showed a faster growth and germination in weak magnetic fields and in the opposite a slower growth in strong ones. Although this mechanism is more difficult to transfer to synthetic systems because on the one hand, it deals with complex effects inside living plants and, on the other, it is very slow because it only affects their growth, this bio-observation shows us that electromagnetic fields can be used to activate morphing depending on the direction of the external field.

These examples illustrate how morphing can be achieved using differential lengths controlled by external triggers, such as light or a magnetic field.

2.3. Pressure and Magnetism

Utricularia or bladderworts are species of aquatic carnivorous plants which also morph to catch preys. It consists of a depressurized chamber with a metastable bilayered trapdoor (Figure 3B). The inner layer presents elongated and radially oriented cells, exerting force on the outside layer made of parallel and smaller cells.[30] The opening by curvature inversion is triggered by preys touching its external hairs, leading to ionic transport in between the layers.[31] This slightly destabilizes the metastable door which releases accumulated stress from internal pressure deformation. Indeed, bladderworts inner parts are depressurized by 17 kPa, thanks to water pumps slowly ejecting absorbed water.[30,31] In addition, this allows the capture movement to be carried out in just 0.5 ms (200 times faster than the flycatcher). The actuation acceleration mechanism is so optimized that it sometimes exceeds the energy threshold, so the bladderwort has to release energy by firing every few hours.

These bladderworts can be a great source of inspiration for the manufacture of morphing devices as movement comes from the combination of pressure, ionic transport, and structured morphology.

More transferable than the previous bio-observation, magnetic fields can also be used to induce movement in plants whose composition contains magnetoresponsive particles. Particle response to external field dispersed in a passive matrix can exert a sufficient force to morph the whole system. Either the dispersion or the field must be heterogeneous. In flax, intracellular amyloplasts are diamagnetic and can move inside the cells under an external magnetic field. In a field gradient, this intracellular movement can lead to macroscopic morphing.[32] Similarly, a grass grown on an iron-rich soil showed to embed in its cells ferrimagnetic iron oxides Fe_2O_3 with two different morphologies.[33] If the distribution of these two different microparticles is not homogeneous, morphing can be initiated in a homogeneous external magnetic field. These observations on specific living systems with an external field are yet another example of how nature has preceded scientists.

These systems highlight the strong potential of dispersing responsive additives in a layer of a passive material to control the actuation of shape morphing devices.

With adaptations for survival of the species through growth, reproduction, or feeding, plants have evolved developing abilities

of morphing activated by various triggers. Several environments led to a lot of passive or active strategies responsible for autonomous movements. In this section, we detailed the main mechanisms developed by the nature to bring shape adaptability. We will illustrate in the next sections how these strategies have been translated to fabricate bioinspired morphing multimaterials, or at least that nature had preceded scientists for some of them.

3. Hygromorph Biomimetic Systems

Inspired by plants dispersing seeds or feeding themselves thanks to autonomous shape change via differential swelling, sometimes based on osmosis between layers, hygromorphs are materials capable of morphing through a gradient of water uptake in- or out-of-plane. The simplest systems are designed with chemically different layers, like pinecone. More advanced systems include differential swelling via a cross-link gradient obtained during processing or afterwards. Advantageously using stimuli-responsive polymers, the shape change can be post-triggered by tuning the temperature or the pH of the solution, or by light and voltage.[34]

3.1. Opportunities and Challenges

Just as pinecone scales, the most straightforward and obvious strategy to obtain a differential swelling is to overlay two chemically different materials of different hydrophilicity leading to humidity-driven morphing. Immersion in water (or contact with moisture) of such bilayer thus triggers the immediate shape change due to the rapid swelling of the more hydrophilic layer.[35,36] In order to get additional control of the morphing thanks to other triggers than immersion, e.g., variation of pH or temperature of water, stimuli-responsive hydrogels are advantageously used to build the active layer. These systems are described in more details in the following sections.[35,36]

Besides, in order to get control over the rate of morphing response and delay the actuation, it is possible to temporally control the rate of water uptake in the active layer. For instance, by using the progressive hydrolysis of a hydrophobic poly(succinimide) layer into a hydrophilic poly(aspartic acid), the shape change can occur progressively over a period of 9–15 h after water immersion.[36] Controlling the rate of actuation is particularly of interest for applications targeting cells encapsulation allowing to give time for cell adsorption before folding to trap them. Conversely, shortening the response time (≈1 s) below the limits of purely diffusive process is made possible getting inspired by the *Dionaea muscipula* leaves, creating hygroscopic bistable structures.[37] These were obtained by bonding pre-stretched polydimethylsiloxane layers prior to depositing hygroscopic electrospun polyethylene oxide nanofibers.

The main challenge of all these bilayer systems is to properly attach them together to prevent delamination upon water uptake. It can be achieved by incomplete cross-linking of the first layer before spraying the other on top, allowing the chains to entangle, and then cross-link them together via compatible reactive functions as in self-healing materials.[38] With fibrous layers instead of bulk gels, fibers intertwining facilitates the interlayer adhesion.[35]

An efficient strategy is to design composite materials with a common matrix throughout the entire thickness and different fillers distribution driving the properties of each layer, like wheat awns (**Figure 4**A).[39–41] This versatile strategy allows to obtain more complex shapes by playing on the distribution and the orientation of the fillers.[39] Even with complex composite structures, Timoshenko's equation generally predicts the optimum ratio of thicknesses of each layer for strongest shape change as well as calculate the resultant curvature based on the ratio of Young moduli.[40] Nevertheless, Ionov's group evidenced that in some complex 3D-printed shapes, uncontrolled folding can occur due to inhomogeneous rate of water diffusion between edges and faces. The obtained rolled shapes upon swelling are statistically dependent on the aspect ratio, which is the ratio between the width and the length of the dry object.[42] At high aspect ratios, the long side rolling is energetically favored due to more consequent water diffusion from the long edges. Though, using fibrous fillers can completely change this and favor the opposite short side rolling, thanks to a fiber direction restriction.[41] For aspect ratios equal to 1 (square shapes), it is either a diagonal rolling for small samples or all-side rolling for large samples (Figure 4B). When the shapes have several foldable arms, it might hinder the complete shape change and lead to multiple statistically distributed final shapes in function of which arm folds first, possibly restricting the neighboring arms.[43] On square samples, favorizing one side was achieved by simply puncturing the gels.[44] The shape change can then be predicted by the geometry, size, and essentially spatial distribution of the holes (Figure 4C). With a central tilted square hole, interesting antisymmetric curvatures paired by opposite corners were obtained. Combining printing methods and composite materials enables the obtention of extremely sophisticated orchid-like shapes after swelling of a flat sheet containing several domains.[45] Indeed, printing can be used to impart anisotropic distribution of fillers, by shear-induced alignment of cellulose fibrils for instance, thus swelling more in perpendicular direction than in the parallel one.

One other scenario is that instead of being laminated, the layers can be attached by one edge. Interestingly, it affects the obtained shapes due to different constraints. Upon swelling, the restrictive layer will not allow folding but will induce a sinusoidal buckling of the free edge of the active layer, resembling the edge of salad leaves.[46] The wavelength shape can be predicted and is mainly tuned by the width of the active strip.

All of these examples above give an overview of the main principles of the hygromorphs, bioinspired from pinecones and wheat awns. In the following, we will show how to further impart a smoother gradient of swelling to overcome the limitations of chemically different bilayers.

3.2. Patterning Various Cross-linking Densities in Hydrogels

To ensure fast response and good adhesion between the active and resistive layers of the hygromorphs, the easiest way is to cross-link chemically similar layers. The gradient of swelling will then be obtained by imparting a different cross-linking density. In a hydrogel sheet, this cross-linking pattern can be achieved out-of-plane via either a peri-process with several strategies or

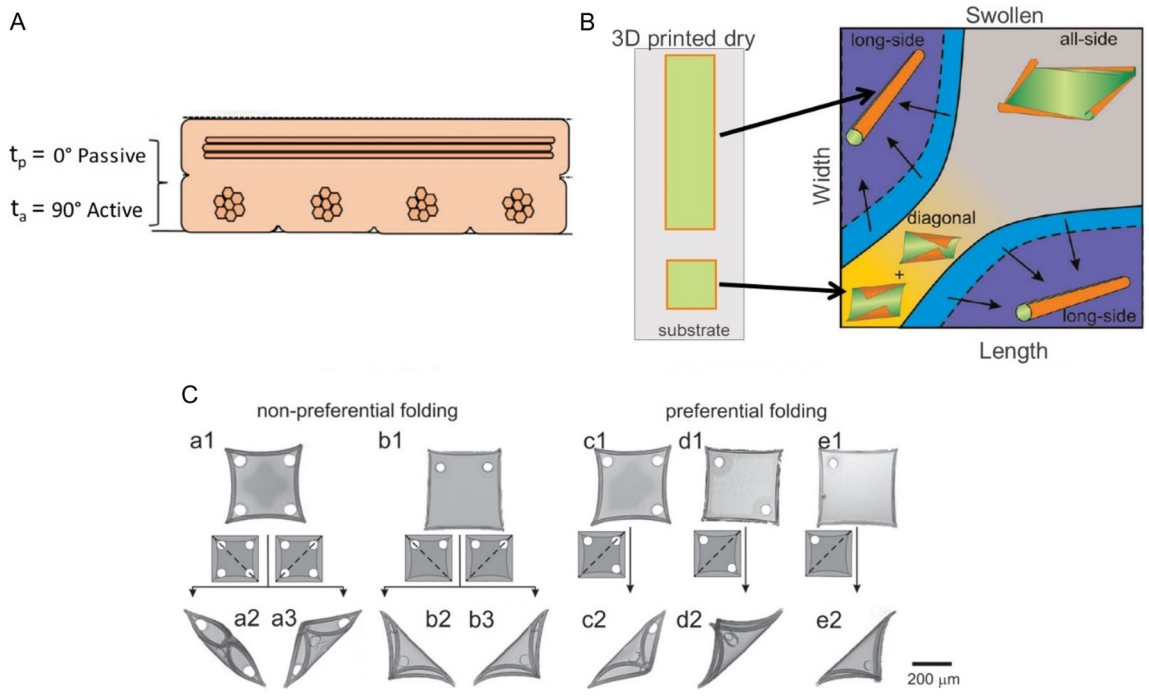

Figure 4. A) Bilayer with perpendicular inserts [Reproduced under the terms of the CC-BY 4.0 license.[40]], B) rolling diagram after swelling based on aspect ratio of the dry object 3D-printed on a substrate [Adapted with permission.[42] Copyright 2024, American Chemical Society], C) restricting folding with controlled punctures [Reproduced with permission.[44] Copyright 2024, Wiley].

post-process with the so-called ionoprinting process, as well as in-plane with a micropatterning design.

3.2.1. Peri-Processes for Out-of-Plane Patterning

The out-of-plane cross-linking gradient in between layers of similar chemical nature is achieved through several strategies. Though, each time the starting point is to mix polymer precursors bearing functions reacting with a cross-linker or bearing polymerizable unsaturations irreversibly cross-linking chains together under UV. The easiest one is to sequentially print the layers of the same polymer with macromolecularly engineered chains to control the molecular mass in between the cross-links. Indeed, spacing the nodes by having different length of polymer chains which are end-capped by cross-linking moieties will enable to tune the crosslinking density, thus the water uptake of each layer. To make it even more straightforward, this system was implemented with commercially available polymers: namely poly(ethylene glycol)-diacrylate (PEGDA) and some dental resin from Zhermack made of poly(vinyl siloxane).[47–49] For instance, with two layers of 200 μm each, the radius of the tube obtained after swelling goes from 9 to 0.7 mm if the PEGDA molar mass of the loosely cross-linked layer goes from 1000 to 10 000 g mol^{-1} (**Figure 5**A).[47]

One other straightforward possibility to impart a cross-linking gradient is to smoothly dose the curing exposure to the sequentially added layers of resin. A report shows that a UV exposure of 2, 3, and 4 s to the first, second, and third layer, respectively, leads to strongly folded structures of poly(N-isopropylacrylamide) (PNIPAM) because the two seconds exposed layer swells by a ratio of 380%, whereas the four seconds exposed layer swells by a ratio of 230%.[50] Nevertheless, with such a small amount in the difference of UV dosage, it was here necessary to add a radical scavenger to avoid the diffusion of cross-linking species when the fresh precursor is added. In some systems, this constitutes a real limitation. Differential dosage of UV can also occur spontaneously when the first cross-linked polymer layer acts as a photomask for the second. Too thick or too heavily cross-linked layers can cause this effect or it can be inherent from the chemical nature of the polymer. This is observed for alginate and hyaluronic acid even though the targeted thickness is only tens of microns.[51] In this study of Ionov's group, the very high degree of methacrylation leads to extremely high cross-linking density, probably increasing the UV absorption. Interestingly, it is the opposite for PEGDA, as shown by Gracias' group; UV absorption is more important in the loosely cross-linked layer.[48] This might be explained by the higher crystallinity for this layer made of longer chains. This strategy was used recently with methacrylate functionalized silk-fibroins in solutions mimicking the in vivo conditions.[52] It is worth noting that this was successfully tested in vivo as a trachea substitute, where the curvature of the innate trachea was obtained through morphing via differential swelling of a gradually cross-linked material. However, in our opinion, precisely controlling the UV-induced chemical reactions remains difficult, such that sample to sample reproducibility might be more challenging.

Crystallinity in polymers was also used to impart a gradient of cross-linking density as it adds up physical cross-links, as exemplified by poly(dimethylglyoxime-urethane) elastomers.[38] The same precursor was used for two layers, but only one layer

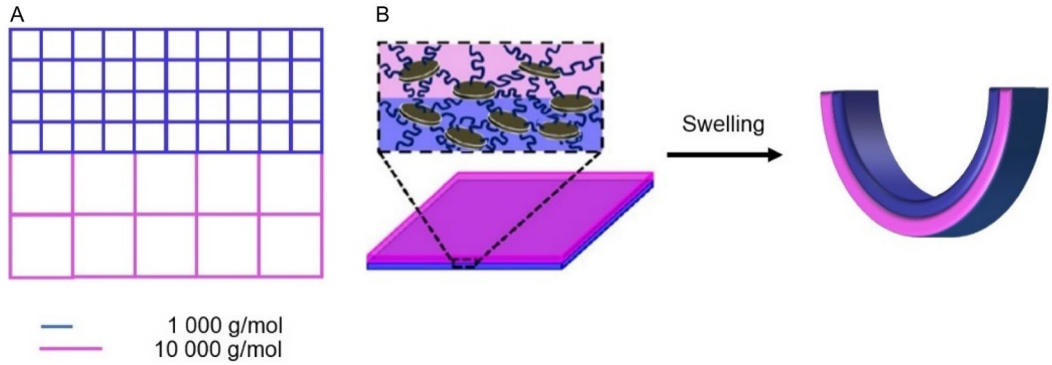

Figure 5. A) Macromolecularly engineered bilayer network, B) heterogeneous clay insertion to bind chains [Adapted with permission.[53] Copyright 2024, American Chemical Society].

was further irreversibly covalently cross-linked, while the other was only having the physical cross-links, creating a gradient.

Similar to crystallinity, another noncovalent bonding can be added through fillers interacting with the chains in the network (Figure 5B). Simply tuning the number of bonding moieties on the chains will affect the crosslinking density. Thus, with two layers of mixture only differing by the amount of polymer functions to bind through the thickness will give a morphing material via differential swelling. This has been done by dispersing clay nanosheets in a poly(N-isopropyl-co-acrylamide) (poly(NIPAM-co-AM) matrix.[53] Interestingly, here clay nanosheets served a double purpose: morphing and reinforcing the material, leading to high tensile strength and stretchability without delamination. Yet, this strategy was possibly difficult to control the distribution of the filler, limiting the obtained curvatures.

More complex shapes could be obtained by spatially controlling the increase of cross-linking density. It was recently explored by a post-process local insertion of chemicals in cross-linked networks. In addition, because the insertion is made once the network is already obtained, it could be designed to be reprogrammed more easily.

3.2.2. Post-Processes for Out-of-Plane Patterning

One very elegant and recent strategy to impart a nonpermanent croslinking gradient post-process is the ionoprinting. Indeed, the first example of such post-processing for morphing dates back from 2013 only. It relies on the localized increase of crosslinking density via a reversible complexation of the polymer chains with ions which have been injected through electric fields in between two electrodes placed on each side of the polymer network (**Figure 6**A).[54] Thus a pattern of higher crosslink density close to the electrode leads to a local decrease of swelling compared to the rest of the gel which has not been ionoprinted and is finally responsible for folding. The main advantage of this strategy compared to the others is that it can be completely reset (Figure 6B). Indeed, the injected ions can be removed by immersing the folded gels in a solution with a chelator agent (ethylediaminetetraacetic acid) which will complex the ions and release the local increased crosslink density. As the complex can be rinsed out, the reprogramming does not suffer from performance loss.

Studies focused on the effect of the obtained curvature in function of the duration of ionoprinting and the strength of the electrical field, as well as how to reinforce, sequentially activate and control the folding direction of such gels.[55–57] The curvature angle was shown to increase with the duration and voltage even though it reaches a plateau. Sequential actuation can be achieved by printing ferric ions (Fe^{3+}) forming tris-complexes and later reducing them into ferrous ions (Fe^{2+}) to partly break the complexes and release some of the local constraint inducing a different folding.[56] The rate of unfolding can be adjusted by the concentration of the reducing solution. Therefore, sequential folding into cubes was obtained with several ionoprinted hinges (Figure 6C). Moreover, the folding direction can be tuned by implementing multilayers sequentially ionoprinted. It will depend on the location of the ionoprinted hinges, inside at the interface between layers or toward the exterior.[57] Different ions are available for ionoprinting if one uses the catechol complexing moieties instead of more classical negatively charged units such as sodium acrylate or phosphate. Complexes of catechol with ions of zinc (Zn), aluminum (Al), and titanium (Ti) were studied and compared to iron (Fe) and cupper (Cu).[58,59] The curvature follows this scheme: $Ti^{4+} > Fe^{3+} > Al^{3+} \approx Cu^{2+} > Zn^{2+}$, meaning that the curvature obtained by injecting Ti^{4+} is stronger than the curvature obtained by injecting Fe^{3+} etc. This rule can be used to impart complex shapes with several curvatures. The extreme titanium ions are really distinguishable from the others. It has the advantage to be more inert but demands higher voltage to be printed and cannot be removed with EDTA once inserted because the formed complex is too stable.[59] Removing it might demand stronger chelation agents which could be detrimental in other ways, and as such it cannot be reprogrammed. On the same principle, it is also possible to inject ions through an electrolyte and using a heterogeneous external field to induce differentially cross-linked shape-adaptable materials.[60]

Perhaps inspired by ionoprinting, another strategy of post-process nonpermanent crosslinking gradient was reported in 2021, based on dimerization and cleavage of moieties (Figure 6D). Coumarin was used as dimerizing unit under 365 nm light and cleavable under 250 nm irradiation.[61] Though, up to now, this system has a loss of capacity through cycling because of asymmetric cleavage of coumarins, but others photocleavable moieties exist and could limit this issue.

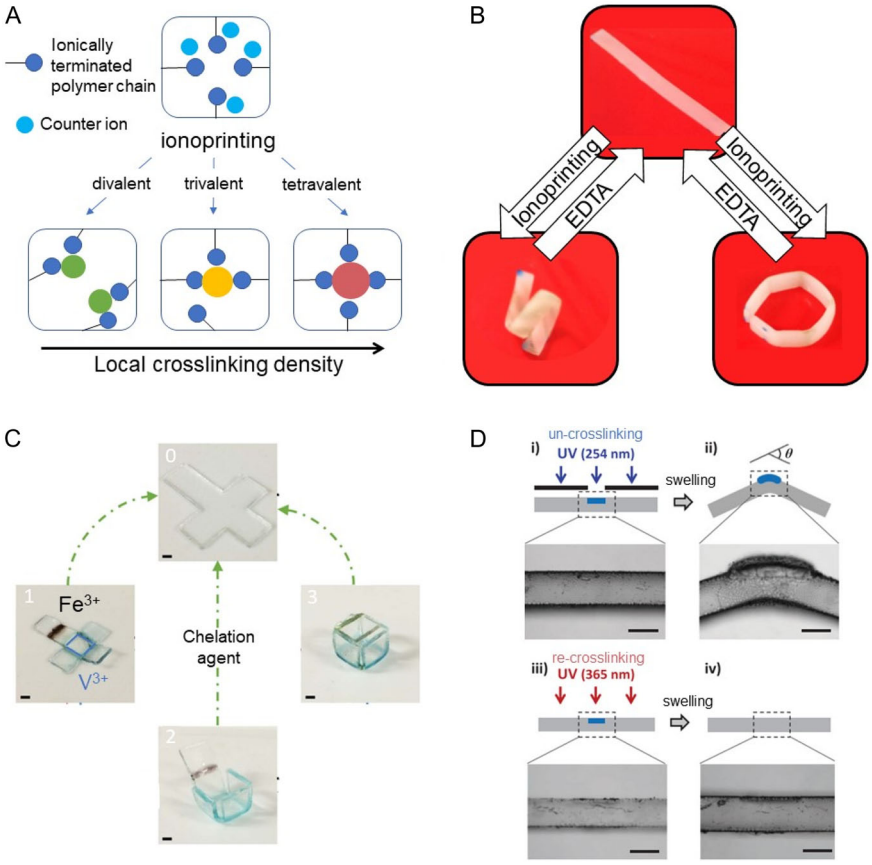

Figure 6. A) Principle of ionoprinting to locally increase the cross-linking density based on multivalent counter ions, B) complete reset of ionoprinting [Reproduced under the terms of the CC-BY 4.0 license.[55]], C) sequential folding on differentially ionoprinted hinges [Reproduced under the terms of the CC-BY 4.0 license.[56]], D) locally un-cross-linking and re-cross-linking through sequential UV-C and UV-A irradiation of coumarin-based hydrogels [Reproduced with permission.[61] Copyright 2024, Wiley].

Nevertheless, even if sequential folding to give 3D objects can be obtained easily with these techniques, even more complex shapes are foreseen through a continuous gradient. This is achieved via an in-plane gradient, meaning that the gradient is not anymore along the thickness but in the plane of the initially flat object.

3.2.3. In-Plane Patterning Processes

In-plane cross-linking gradients warrant much more complex shapes as the gradients can be smoother, more localized and alternated inducing wider possibilities for shape change. Hayward's and Santangelo's groups first photo-crosslinked PNIPAM with a photomask consisting of hexagonal dots of tens of microns.[62] The holes in the mask were responsible for an alternating pattern of highly cross-linked dots receiving a UV dose of 13.9 J m^{-2} and loosely cross-linked areas receiving a UV dose of 0.2 J m^{-2} (**Figure 7**A). This in-plane gradient between dots swelling differently with a fourfold factor leads to hemispheres, saddles, cones, and Enneper's surface depending on the distribution of the dots (Figure 7B). More recently, they used a digital micromirror array device (DMD) to even more precisely control the dose (down to 1.37 µm) for smoother transitions imparting smoother 3D shapes.[63] Indeed, they were able to print the equivalent of 256 patterns, from exterior to interior to have a very linear gradient. It is equivalent to use 256 photomasks, which would be very tedious. However, with such dome-like shapes, multiple metastable configurations can step in, especially when several ones are printed side to side on a same sheet (Figure 7C). For instance, with three side to side patterns to obtain domes, there are three independent possible shapes namely all domes pointing on the same side, two consecutive domes on one side and the third one on the other side, and alternating sides. To make the sheets preferentially morph in domes all oriented on the same side, they added a photo-absorber to add up a small gradient out-of-plane by decreasing the penetration depth of the UV light.[64] Finally, another study showed that this digital in-plane patterning could be used with a monomer mixture as precursor instead of already polymerized chains, lowering the process cost because one step is bypassed.[65] They demonstrated complexity in the swollen shapes such as a smiling face with polyacrylates. It is worth noting that they used visible light and times of exposure varying between 12 and 24 s, here again increasing the cost-effectiveness of their procedure.

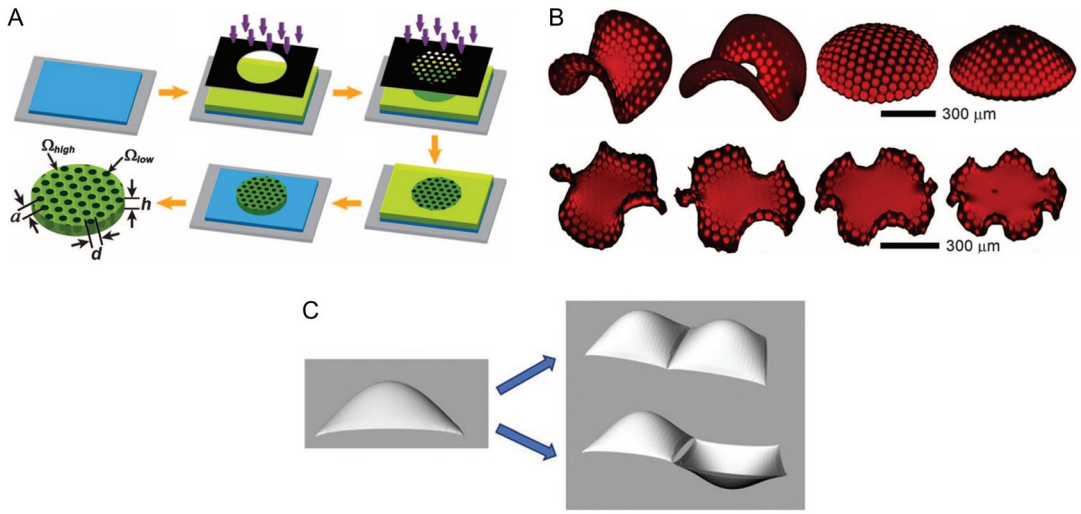

Figure 7. A) Principle of in-plane gradient of cross-linking with dots patterned photomask [Reproduced with permission.[62] Copyright 2024, American Association for the Advancement of Science], B) obtained shapes from various dots distribution [Reproduced with permission.[62] Copyright 2024, American Association for the Advancement of Science], C) multiple possibilities for dome morphing [Reproduced with permission.[64] Copyright 2024, Wiley].

This cross-link density gradient strategy has several advantages such as using mono-material while obtaining extremely complex shapes with processes lasting only few seconds to few minutes. However, in the reported examples, the vast majority morph straight away once immersed, and needs a prolonged actuation. For shape-adaptable systems, there is also a need to control the transition by means of a temperature, pH, light, or voltage trigger which is possible with functional hydrogels.

3.3. Triggered by Temperature or pH

When the hydrogels are thermo- or pH-responsive, the morphing can be temporally controlled. Responsive swelling or shrinking of some parts is used to obtain differential swelling within the material.

Most of the thermo-responsive actuators use a polymer displaying a lower critical solution temperature (LCST) above which it becomes immiscible to the solvent. When networks (IPN or chemically cross-linked gels) are made of this kind of polymers, they swell at a temperature below the LCST and shrink by expelling the solvent out of the network above the LCST. The most studied thermo-sensitive polymer is the PNIPAM notably because its LCST at 32 °C is between room temperature and body temperature (**Figure 8**A) and can be slightly tuned by copolymerizing NIPAM with other monomers. The easiest way to use PNIPAM for shape change is to have a bilayer system with one layer made of PNIPAM and the other one of a passive polymer such as poly(methyl methacrylate) (PMMA).[66] As a consequence of shrinking, PNIPAM is found at the interior of the folded shape when the water temperature is raised. It usually swells back below the LCST, restoring the starting flat sheet (Figure 8A). Therefore, shape reversibility is preserved. Interestingly, the folded shape can be fixed even if the temperature is decreased by encapsulating oil, the high surface tension between oil and the PNIPAM layer preventing its unfolding below the LCST (Figure 8A). Moreover, the rate of deswelling of PNIPAM can be tuned by the amount of cross-linkers. PNIPAM-PNIPAM bilayer systems with different cross-linking agent fold due to different shrinking rates, but ultimately restore the flat shape upon complete deswelling of both layers.[53]

PNIPAM was also 3D-printed with anisotropic fillers to reinforce it, as well as electrospun fibers.[67,68] Electrospun PNIPAM fibers cross-linked during electrospinning to maintain the fibrous morphology present the advantage such as porous systems in general of absorbing more water, enhancing the movement by the larger difference between swollen and shrunk states. The porosity also induces a faster response. Accordingly, porous and bulky PNIPAM bilayers were obtained by a one-step process called evaporation-induced concentration differentiation.[69] The high porosity of one side enabled rapid and important shrinking above the LCST and thus a 1080°-folding in only one second. Moreover, similar to one strategy for inducing a cross-link gradient post-process, a monolayer gel with NIPAM copolymerized with another monomer bearing coumarin functions were partially uncrosslinked and morphed upon increasing water temperature.[70]

The thermo-response can also be triggered with polymers not displaying a LCST or thermo-sensitive ones other than PNIPAM. A bilayer of electrospun poly(ε-caprolactone) (PCL) and poly(lactic acid) (PLA) did not roll in water at 20 °C and self-folded at 40 °C.[35] This was due to further shrinking of PLA, thought to be coming from a water plasticizing effect and a water temperature close to the glass transition temperature (T_g) inducing partial chain movement releasing some stress accumulated by the fibrous morphology.

Interestingly, the LCST of poly(N-vinylcaprolactam) (PNVCL) can be controlled by the cross-link density, and a bilayer system with poly(dimethyl siloxane) (PDMS) was demonstrated to bend upon water temperature increase.[71] Other examples are poly(N, N'-diethylacrylamide) (PDEAM), which is a softer hydrogel than

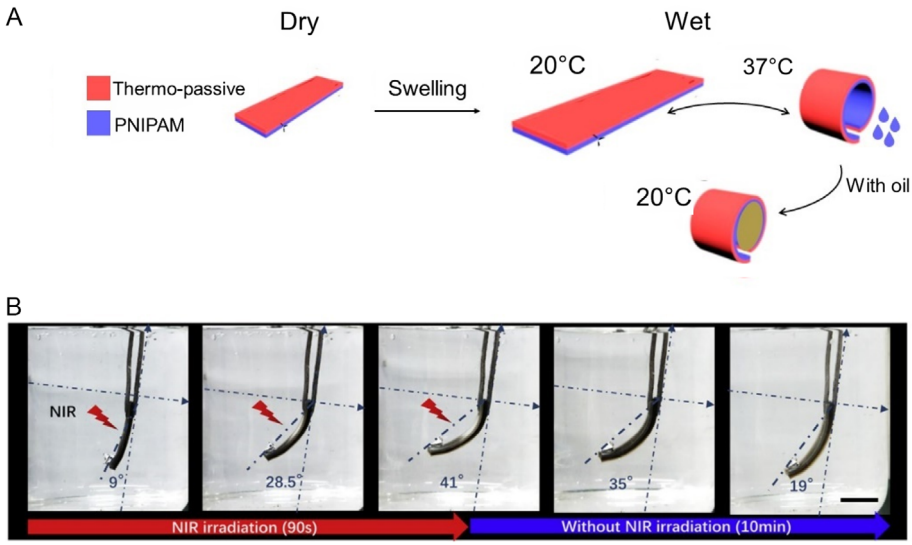

Figure 8. A) Principle of a thermoresponsive hygromorph and oil strategy to lock the fold [Adapted with permission.[68] Copyright 2024, American Chemical Society], B) principle of NIR actuation by localized heating [Reproduced with permission.[81] Copyright 2024, Elsevier].

PNIPAM and poly(2-(dimethylamino) ethyl methacrylate) (PDMAEMA) which LCST depends on pH.[64,72] Both are advantageously used in shape-changing materials.

Similarly, tuning the pH of the solution can lead to differential swelling/shrinking when pH-sensitive units are introduced on one side of a bilayer system. This is described for poly(hydroxyethyl methacrylate) (PHEMA) and poly(acrylic acid) (PAAc), which swells in basic media upon deprotonation of the carboxylic acid functions.[73]

In systems where both layers are pH-responsive at a different pH, folding in both directions is achieved.[74] Finally, more complex 3D shapes were obtained by pH-triggered delamination of layers by decoupling β-cyclodextrin and ferrocene moieties attached to the chains of each layer respectively.[75]

Remarkably, pH- and thermo-responsive materials were combined together to allow reaching several shapes. Indeed, controlling the pH (low or high) and the temperature (below or above LCST) leads to four different shapes.[76] For example, manufacturing a trilayer of one passive, one thermo-responsive, and one pH-responsive layer with common polymers (PCL, PNIPAM, and PAAc) is straightforward.[77] In addition to folding in different directions, folding along the long or the short side is controlled by the solution parameters.

Besides, multiresponsiveness can be achieved by two thermoresponsive layers among which one has an LCST controlled by the pH.[72]

Moreover, even though it is not, strictly speaking, actuated by pH in the sense that pH does not induce the folding of the sheet, we thought interesting to highlight a strategy where a bilayer is morphing upon thermal trigger, and this deformation is fixed by tuning the pH inducing the micro-crystallization of chitosan moieties attached to the chains.[78] Thus, it prevents unfolding when the temperature of the solution is lowered back but can unfold lowering the pH again. This double feature is highly handy to sequentially trigger the system and for shape locking while changing the solution parameters.

Even though the temperature of the solution can be tuned whenever it is needed to trigger, it induces an overall response of the entire body. It could be extremely valuable to localize the heating to impart easily complex shapes of several curvatures. For that purpose, light was used to locally heat parts of the body.

3.4. Triggered by Light

Light is an indirect trigger because it enables to locally heat, but the mechanism lying underneath the folding is the same as to tune the solution temperature inducing differential swelling. It presents the main advantages to be a localized and remote trigger (Figure 8B). We will focus on NIR irradiation here because at these wavelengths light can go through layers of soft matter such as body tissues without damage. It is one of the reasons why NIR actuators were more deeply investigated, especially for biomedical intelligent devices where NIR light can precisely and locally heat specific parts of the body without perturbing the whole medium. Three different strategies are cited here among the most recent studies.

First, conductive polymers that absorb light in a wide range of wavelength are efficiently used as interpenetrated networks or as one of the layers in bilayer sheets. For instance, polyaniline (PANi) was embedded in a double network of PNIPAM and poly(vinyl alcohol) (PVA) to form the active layer, while the passive layer was made of poly(acrylamide) PAAm.[79] PANi serves as a photothermal convertor allowing transition to the folded shape. Nevertheless, PANi being highly heat conductive, the surface reaches easily 60 °C upon NIR exposure, which could be detrimental to several applications, for instance when cells are involved.

Several photothermal converters were successfully embedded and homogeneously dispersed in thermoresponsive polymers. These fillers are organic or inorganic micro- or nanoparticles such as PPy nanoparticles, graphene oxide (GO), graphene, multiwalled carbon nanotubes (MWCNTs), transition metal carbides

(MXenes), and gold nanorods (AuNRs). Monodisperse nanoparticles (90 nm) of PPy were embedded in a PNIPAM heterogeneously porous matrix, the high porosity enhancing the loading.[80] GO was homogeneously dispersed in PNIPAM by sonication and then laminated to either poly(N,N-dimethylacrylamide) (PDMAA) or PEGDA.[81,82] Interestingly, such light-controlled folding bilayer was successfully used for opening a valve which was achieved in 1990s, while the recovery after stopping irradiation took 10 min. This could be used for sequential folding with only one light source.[81] Graphene was similarly embedded in PNIPAM to design a system able to grip a single cell of 10 µm and to impart movement.[83] The lever movement was achieved by the shrinking of the PNIPAM-graphene monolayer perpendicular to two photoresistive arms that actuate the gripping.

Moreover, MWCNTs were successfully inserted in a bilayer with PNIPAM. Though, it is worth noting that the MWNCTs were added in the passive layer for color purpose, the heat transmission was efficient enough to morph the hydrogel.[84] The drawback is that, here again, the surface of the sample reaches 50 °C. MXenes were used both as a photothermal agent and as inorganic cross-linker leading to a light-sensitive biocompatible layer folding by 180° in 1980s.[85] Finally, gold nanorods were also embedded in PNIPAM to give morphing abilities. With the optimal aspect ratio (length/width) of 4.12, AuNRs reached a photothermal conversion of 45% decreasing the intensity of NIR needed down to 1 W cm^{-2}.[86] AuNRs are also highly interesting for their rapid and reversible actuation (10 Hz) preventing the actuator to heat over 39 °C, i.e., the temperature of heat shocks for living cells.[87]

Light proved to be a very interesting option to initiate the shape change, though it is difficult to obtain multi-directional morphing. Therefore, hygromorphs triggered with voltage, by placing them in between two electrodes, were developed.

3.5. Triggered by a Voltage

Electroactive hygromorphs (EAHs) are electrically charged hydrogels such as polyanions or polycations which shape change when they are immersed in an electrolyte solution (NaCl solution, phosphate buffered saline (PBS), DMEM, etc.) and placed in between two electrodes. The bending direction depends on the direction of the electric field, thus can be reverted as illustrated in **Figure 9**A. The differential swelling responsible for bending is achieved in a mono-layer material by differential osmotic pressure resulting from the movement of mobile ions inside the gel (Figure 9A). Though the exact mechanism is still debated, the main ones are properly discussed in a recent report from 2022.[88] The voltage-dependent bending degree was already quantified in 1990 by Tohru Shiga and Toshio Kurauchi who established the following equation: $Y = \frac{RTC_p L^2 h_{ions} t(1-h_{ions})}{DE}$ with Y is the bending degree, R is the gas constant, T is the temperature, C_p is the concentration of cations, L is the length of the hydrogel before actuation, h_{ions} is the migration rate, t is the duration of electric field actuation, D is the thickness of the hydrogel, and E is the Young modulus at the swollen state.[89] This generic equation applies to all the materials used for such EAHs, offering a wide variety of available hydrogels ranging from synthetic polymers to biosourced polysaccharides. With this strategy reversibility between two shapes is easily obtained, and ion movement is sufficiently harmless to limit the performance loss upon cycling.

One of the most widely used polyanion, inevitably studied for EAH is PAAc. Thanks to its 3D-printability, complex shapes of this hydrogel are achieved. Up to now, it is one of the only materials reported to be used as an actuator such as a gripper (Figure 9B) even if high voltages (up to 30 V) are needed for

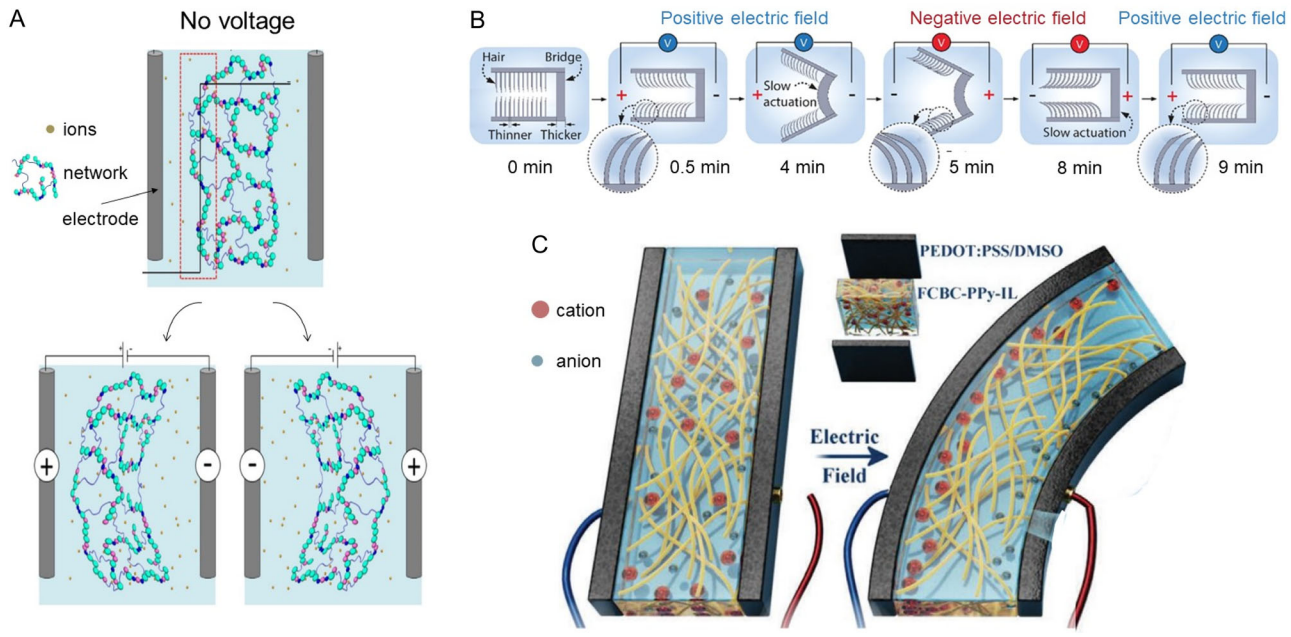

Figure 9. A) Principles of reversible electroactuation [Reproduced with permission.[95] Copyright 2024, Elsevier], B) gripper with differential movement due to faster/slower response based on thickness [Adapted with permission.[90] Copyright 2024, American Chemical Society], C) hygromorph sandwiched between flexible electrodes [Reproduced with permission.[97] Copyright 2024, Wiley].

deformations limited to 43°.[90,91] Other synthetic systems include monomers like 2-acrylamido-2-methylpropanesulfonic acid sodium salt (AMPS) as well as 4-vinylbenzenesulfonate (Na4VBS) copolymerized with HEMA or acrylonitrile (AN) and AAm to balance hydrophilicity and mechanical properties.[92–95]

However, such charged polymers are intrinsically mechanically weak due to electrostatic repulsion between chains inducing low entanglement. Thus, PAMPS was reinforced with particles of pluronic F127 diacrylate acting as a cross-linker without preventing ion movement and actuation in electrical fields. [95-Intro128] Interestingly, P(Na4VBS) could be actuated at lower voltages compared to PAAc and PAMPS, down to 1 V with a bending speed of 2.7° s^{-1}.

Moreover, biosourced polysaccharides were intensively studied for EAHs. Examples with chitosan/carboxymethyl cellulose, functionalized carboxylated bacterial cellulose (FCBC), sodium alginate, and pullulan were published in the last five years.[88,96–98] Among these, FCBC presents the advantage to be actuated at voltages as low as 0.5 V with a complete folding in maximum 4 s.

In 2022, Lacey Reid and Wadood Hamad made a breakthrough by inserting bio-sourced cellulose nanocrystals (CNCs) later sulfonated in non-electroactive matrices.[99] This could then turn almost all non-electroactive polymers in electro-triggered actuators (ETAs) and opened up a new path for new composites in the field of ETAs.

Finally, as plants that do not necessarily need complete immersion in water to morph, studies evidenced that voltage folding is still possible when the hydrogel is removed from the medium. These studies proved that movement of ions from outside into the gel is not absolutely required to achieve actuation and bending, just like how it is done in nature. It was demonstrated by preventing water to flow out of the hydrogel, like in Venus flytraps where the water movement is internal. It was performed either by sandwiching the gel between flexible electrodes (Figure 9C) or immersing the swollen hydrogel in an oil bath.[97,98] Lastly, it was also shown that water can be replaced by an ionic liquid, namely 1-butyl-3-methylimidazolium tetrafluoroborate ($BMIMBF_4$) by using poly([2-(acrylolyoxy)ethyl] triethylammonium chloride) as electroactive polymer.[100]

Inspired by plants that are able to tune their stiffness and to achieve macroscopic movements generated by water influx due to osmotic concentration gradients, actuators based on osmosis concept originated about 10 years ago. These bioinspired osmosis actuators appear as a less developed area until now, most probably because reversibility was still an open issue hampering its implementation. Even though, a recent paper proposed plant-inspired osmotic actuation that shows reversibility.[101] The strategy, based on electrosorption of ions on flexible and porous carbon electrodes upon application of a low voltage, allows a reversible stiffening of the material leading to impressive actuation with about 500 deg rotation of the tendril-like soft robot. Based on biocompatible materials and low voltage, this reversible osmotic actuator opens new application prospects.

As a general conclusion of this section on hygromorphs, it seems appropriate to us to relate it to the main conclusions of Leonid Ionov in his 2013 review, who also took the position to link hygromorphs with plants in nature.[102] After 10 years, the main innovations focused on getting cross-link gradients, such as iono-printing and in-plane gradients, allowing to impart more complex shapes and multi-curvatures with a unique material,[103] thus a simple strategy ensuring no delamination. We have also tried to dig deeper into the different strategies and materials available for light-activated thermal response, as it is a growing field with many recent papers especially due to large prospects for the biomedical applications with increased safety, easy, and remote trigger.

At this stage, we believe that hygromorphs could benefit in the future from applying new materials in these strategies. For instance, more bio-sourced and/or degradable materials could be used to answer increasingly demanding applications, especially less toxic for users. In the future, more advanced hygromorphs can be foreseen by implementing the cross-link gradient strategy to different trigger responsive systems.

However, hygromorphs are not the only shape-adapting systems, and other advantages arise from other morphing mechanisms.

4. Magnetomorphs

Here, care must be taken to distinguish the hygromorphs triggered by a magnetic field and magnetomorphs. In the first case, the movement is first defined by differential swelling, and the trigger is a magnetic field to initiate the swelling difference. For example, in this case, if the material was free it would only induce movement due to magnetic attraction, and not shape change. For instance, this was used for self-knotting wires.[104]

In the opposite, the magnetomorphs take their names from the mechanism of morphing, where dispersed magneto-responsive particles force the whole material to change its shape. This might be correlated to the intracellular diamagnetism of flax seeds. This mechanism does not require bilayer materials and resembles the in-plane cross-link gradient of hygromorphs. Magnetorheological materials are sometimes referred as magnetoactive soft materials or soft magneto-responsive actuators, and that we will call magnetomorphs in this review to link them to the other classes of morphing mechanisms. They are one of the most thriving classes of smart materials. Indeed, magnetic fields present the advantages of being a remote, safe, and fast trigger with a high penetration in almost all materials and tissues making them especially promising for applications in the forefront biomedical devices as shown in an exhaustive review published in 2022 on magnetic soft robots.[105,106] Herein, we will focus on presenting the mechanism with the main publications and the latest advances in the field, putting these systems into perspective by comparing with the other morphing strategies.

For such magnetomorphs, the spectrum of possible particles is limited to hard magnetic ones with a high remanence meaning that the particles keep their magnetization when the external magnetic field is turned off, and a high coercivity meaning that it can be put in another external field without being demagnetized. Among these, neodymium alloys, such as NdFeB microparticles, are the most widely used for morphing, being commercially available and having high magnetic performances at relatively low cost.

The magnetization to orient these magnetic dipoles in the elastomer matrix, such as silicone elastomers, can be done peri-process or post-process following different strategies. A 3D printer modified with a rotatable magnet allows the magnetization at the same time as the curing of the printed sequence.[107,108] This technique enables to design very complex shapes, as shown in **Figure 10**A, with several domains that can be actuated in 0.1 s and retrieve its initial shape in 0.2 s.[107] Besides, the magnetization for predefining the morphing can be made post-process by inserting the material in a jig and applying a uniform external field (Figure 10B).[109] Thus at rest, the silicone elastomer matrix constrains the material to remain flat which is the shape into which it was cured, and under an external field the aligning dipoles are responsible for forcing the elastomer into the shape defined by the jig.

Since designing a jig for each shape is time consuming, another strategy based on kirigami designs was developed for getting complex shapes by defining them post-process without needing a mold. As illustrated in Figure 10C, this method uses kirigami designs and out-of-plane buckling by temporarily stitching the magnetomorph to a prestressed sheet for magnetization.[110] This temporary buckling of the sheet while magnetized can easily lead to a strong variety of shapes such as faces with all kinds of emotions.

From these complex shape changes, several types of movements can be obtained. Indeed, micro-magnetomorphs were demonstrated to swim, climb, roll, walk, and even jump thanks to actuation of the self-shaping body in contact to a hard surface.[111] It was successfully used ex-vivo to walk toward one object, grasp it, and walk back. This variety of movements comes from one of the main advantages of using a magnetic field as an actuation source, namely its ability to be a directional trigger of controllable orientation and amplitude. Moreover, reversible morphing can be used to move the object. It was done via helical propulsion thanks to an object with a magnetic head and a four times longer nonmagnetic tail under a rotating field.[112] Also, hexagonal plates were twisted under magnetic field and induced the folding of nonmagnetic structures linking them together along predefined creases, like an accordion.[113]

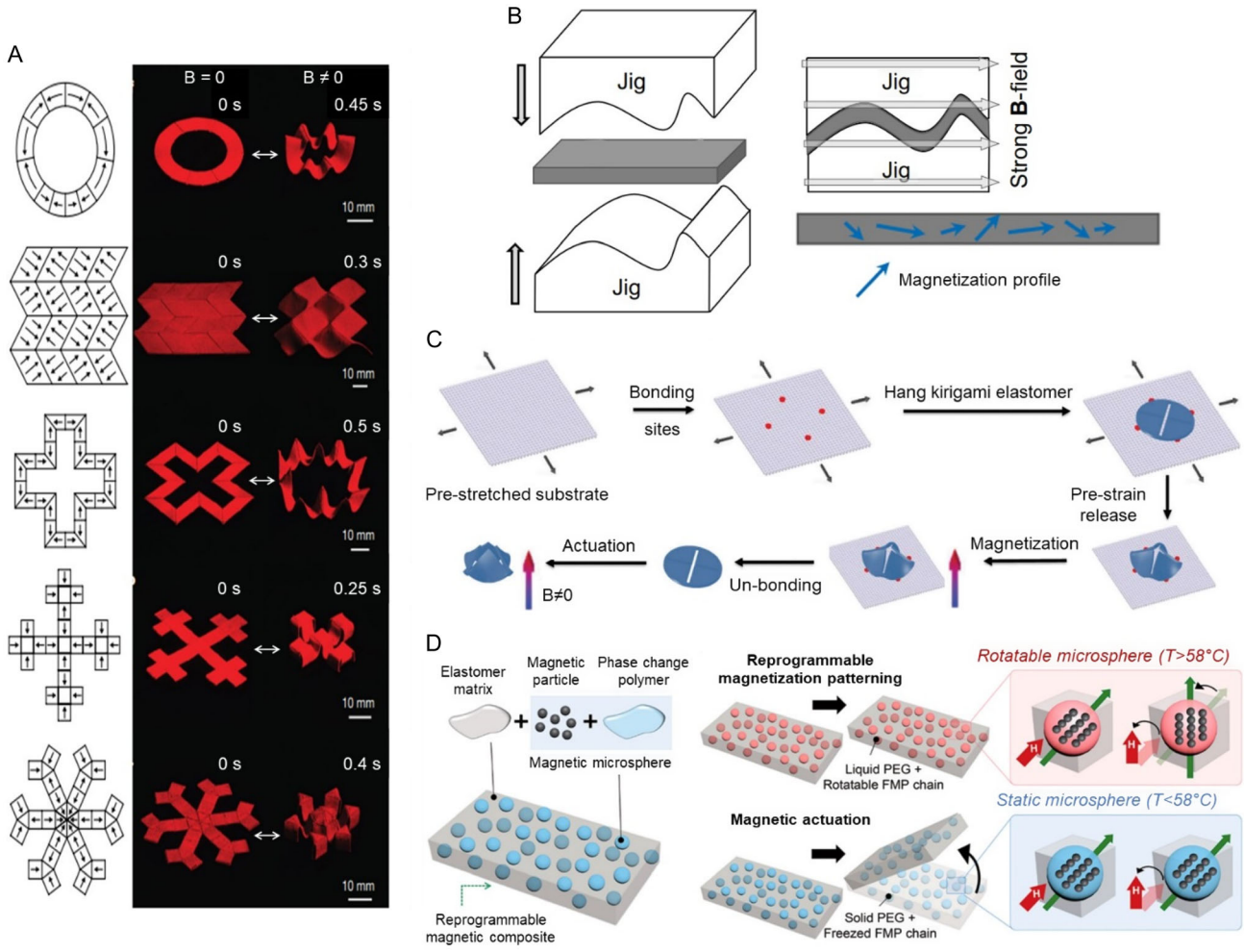

Figure 10. A) 3D-printed domains leading to fast and reversible shape change [Reproduced with permission.[107] Copyright 2024, Springer Nature], principles of magnetizing post-process with B) a jig [Reproduced with permission.[109] Copyright 2024, National Academy of Sciences] or C) a prestretched sheet [Reproduced under the terms of the CC-BY 4.0 license.[110]], D) principle of shape reprogramming with magnetic microspheres embedded in an elastomer matrix [Adapted with permission.[118] Copyright 2024, American Chemical Society].

Most recent advances in the field of magnetomorphs are the shape locking and shape-reprogramming that are worth to underline. The shape locking can be metastable or stable. First, the metastability is achieved through particle attraction from both ends of an object which was sequentially folded in a cube for instance.[114] When the two extremities of such objects get in contact, the external field can be removed and the shape will be kept. It is metastable because a small stimulus could break down this equilibrium and the material could then retrieve its initial shape thanks to the elasticity of the matrix. Semi-permanent shape locking can be designed by going through a transition temperature of the cured matrix, like glass transition (T_g), where the material is hard or soft. Examples used poly(lactic acid) (PLA) and acrylate-urethane copolymers to have a reasonable T_g.[115,116] Indeed, at a temperature higher than T_g, the material is soft and can be actuated with a magnetic field, but when the temperature decreases the material becomes too hard and the shape is fixed. It can be retrieved by heating again the material. Interestingly, this heating can be achieved without an external thermal source. Qi's and Zhao's groups showed that it was possible to embed magneto-thermal convertors such as Fe_3O_4 particles which were responsible for softening the matrix.[116] By varying the concentration of these particles, they achieved a sequential folding where the temperature increases at different speeds. Permanent shape locking was more simply obtained by laminating a material with a plastic behavior such as raw paper for instance.[117]

Shape-reprogramming was very finely executed by dispersing in an elastomer matrix the magnetic particles already dispersed in a matrix able to soften, e.g., PEG4000. The latter is softened by overcoming its T_g allowing these entire domains of particles to realign following the external field and then lock by lowering temperature.[118,119] The procedure of this shape-reprogramming ability is displayed in Figure 10D. Interestingly, in both examples, the intermediate matrix is PEG4000 with a T_g of 58 °C and the particles are either NdFeB or FeCo. For this application, softer particles with a lower coercivity such as FeCo could indeed be interesting to facilitate the reprogramming.

In conclusion, rapid and remote actuation in all media is a clear advantage for hygromorphs. It enables an ultrafast and completely reversible shape-adaptation. It is also based on a mechanism leading to very complex shapes by simple fabrication processes. There is no need for lamination that also makes faster the processes. Though it is a young field and efforts should be clearly made toward the variety of elastomer matrices and magnetic particles accessible. As we mentioned in the introduction of this paragraph, because of the proven safety of magnetic actuation, several applications are foreseen for biomedical systems. Though NdFeB are not necessarily proven to be safe in human interactions and this could limit the applicability toward these applications if efforts are not made to find other magnets. Moreover, as proposed by Lanceros-Mendez's team, future works should focus also on different geometries of particles to maybe impart additional morphing lever than current ones.[120] This could be inspired by the photothermal convertors. Finally, is it interesting to note that exactly like hygromorphs, most recent efforts were made toward reprogramming and shape locking to better control shape-morphing. However, it is rarely mentioned how good is the performance retention with these strategies. Indeed, one could think that a slight alteration of the matrix embedding the particles could have severe impact on the performance. These questions would definitely be worth to investigate.

Despite strong advantages like safety of triggering or variety of simple processes, magnetomorphs require the addition of magnetic particles inside the polymer matrix. Therefore, other strategies to impart shape change at the dry state, without the addition of magnetic particles were investigated, such as mechanomorphs.

5. Mechanomorphs

Bioinspired, notably from cyclamen or sunflower which bend upon a differential growth, mechanomorphs are materials which morph thanks to different residual strains. Typically, bilayers of different elastic recoveries, such as an elastomer laminated with a plastic layer, when stretched, are adapting their shapes upon release of the mechanical stress, since both layers do not fall back in the same manner. After stress release, the layer with the higher elastic recovery will exert a compressive force as it wants to fall back, while the layer with the plastic behavior will exert an extensive force as it wants to maintain its position. These opposite forces along the thickness create a bending moment responsible for the folding. In this part, we will see that like hygromorphs, different triggers are accessible depending on the chemical nature of the elastomer layer. First, we will discuss the most straightforward trigger: mechanical stretching. Then, we will present voltage, temperature and light triggers with the dielectric elastomer actuators (DEAs) and liquid crystalline elastomers (LCEs).

5.1. Mechanical Trigger

The advantage of the mechanical trigger is that it is the most straightforward and simple one. There is no need of complex processes, different media, or expensive apparatus. Indeed, the morphing can be obtained by stretching by hands and release. Moreover, it can be obtained with a large diversity of accessible materials as it only requires two materials of different mechanical behaviors, namely a thermoplastic and an elastomer. The objective of this paragraph is to show that from simplicity, complex morphing can also arise.

The gradient in residual strain even does not absolutely require different materials but can be obtained by structuring a single material. Indeed, a silicone ribbon that is structured to present one bulky layer on one side and one structured layer on the other side will answer differently to the uni-axial stress.[121] The bulky layer will be stretched in the direction of stress and thus compressed in the transverse direction as it is made of a silicone elastomer. In the opposite, the structured transverse ribbons will only be spaced out from each other and no Poisson's contraction occurs. Finally, stretching creates a gradient in the extent of transverse compression along the thickness, which is responsible for folding in the perpendicular direction. Then, the angle formed by the aligned ribbons with the long-axis direction (also the stretching direction) will lead to bending with the structured layer toward the exterior or toward the interior (**Figure 11**A). This could be valuable for several

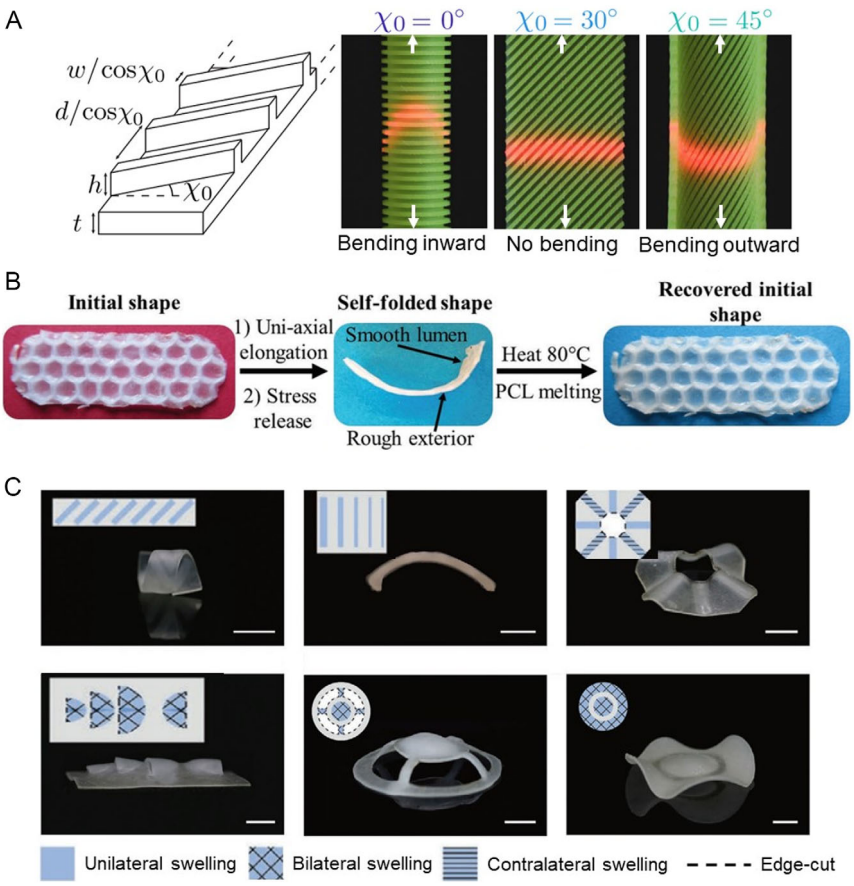

Figure 11. A) Angle-dependent folding of a structured silicone [Reprinted with permission.[121] Copyright 2024, American Physical Society], B) structuration of a semi-crystalline filler for imparting shape locking and shape reprogramming,[130] C) various shapes from differently paraffin swollen materials [Reproduced with permission.[131] Copyright 2024, Wiley].

applications, as one side of the curved ribbon is smooth, and the other is rough. However, the shape change can only be obtained while stretching. As it is made only from elastomer, when the force is released, the material automatically goes back to the flat sheet. The folding upon structuration was also achieved with more complex patterns in-plane, curving again in the transverse direction from the traction direction.[122] Similarly to what is described in Section 3.2.3., controlling the crosslink gradient by controlling the curing dosage can give materials with in-plane variations of mechanical properties and T_g, hence creating hinges along which folding starts. As an example, with acrylates, the gradient in Young moduli can reach three orders of magnitude, and T_g can easily vary in a range of 50 °C.[123]

The gradient of residual strain can also be achieved by laminating two materials with different shape-recovery kinetics upon stress release. It was obtained by tuning the side-chain of 1-alkyl-3-vinylimidazolium tetrafluoroborate ([R-VIM]BF_4).[124,125] The shape recovery is faster when the alkyl chain is smaller. After 6 min, the strain went back from 100% to around 10% for the [1-hexyl-VIM]BF_4, to around 70% for the [1-butyl-VIM]BF_4, and 99% for the [1-ethyl-VIM]BF_4. Helical shapes can be obtained by printing one layer with a tilt from the other one. Interestingly, Nelson's group injected a mechano-chromic agent that changes color sensing when sufficient stress is applied for further bending on release.[125] The main limit of this strategy is that eventually the initial shape will be recovered, then the folded shape cannot be locked.

To enable shape locking, Barone's group used a bilayer of polyolefin thermoplastic elastomer (TPE) at very high strains. One layer is loosely crystalline, and the other is highly crystalline.[126] As TPE are physically cross-linked they can be thermally unstretched to recover the initial shape. Here, is it worth noting that it is one of the scarce examples using such TPE which can be stretched up to 1000% which has never been reached with chemically cured elastomers. Thus, it gives interesting hints on what happens for morphing at such stresses. To sum up, not only bending but also curling and twisting was obtained with isotropic layers which is the only example of non-linear folding without anisotropic inserts. Unfortunately, after such stretching, the system did not completely recover. Poor reversibility prevents the material to be used more than once and could be detrimental for some applications.

In order to impart shape locking and shape recovery (also called reversibility) at the same time, one recent strategy has been to embed fibers of the plastic material in the elastomer matrix, instead of laminating a layer of each material. Such fibers are

locking the adapted shape by plastic stiffness but could be softened by overcoming T_g to recover the initial shape. To ensure the residual strain gradient, either the fibers are not embedded along the whole thickness or two layers are laminated with two different fiber orientations, imitating the structure of *bauhinia variegate*.[127,128] Complex shapes were achieved by locally embedding fibers creating hinges, as for instance miura-ori patterns with mountains and valleys. Though the fibers are very stiff below T_g, and these materials had to be hot-programmed for morphing. With poly(vinyl acetate) (PVAc) fibers, increasing the shape-locking capacity was always detrimental to shape recovery and vice versa.[129]

In our group, we succeeded to optimize those two properties at once by embedding semi-crystalline fibers of PCL in a silicone matrix.[130] At room temperature, PCL being in its leather state, it was possible to cold program the shape-change. We used both advantages of the presented structuration and the strategy to shape locking and shape recovery by using a honeycomb pattern of electrospun fibers (Figure 11B).

In addition to shape locking and shape recovery, shape reprogramming is also a recent concern for mechanomorphs. One very recent example showed that it was possible to embed, after the process, a crystallizable molecule by swelling with masks when molten, and remove it by swelling in a solvent. Luo's group used paraffin in a polyacrylate elastomer and hexane for shape-reprogramming.[131] Indeed, upon swelling in hexane, paraffin is completely removed and could be reinserted in a different pattern to achieve different shapes upon stress and release. Various shapes were reached by swelling on one or both sides, during different times, and in different patterns with masks as shown in Figure 11C.

Even though it presents simplicity and efficiency to obtain the shape-change, it could still be important for other applications to trigger differently the mechanomorphs. This was achieved by DEAs with electric currents and LCEs with light or temperature.

5.2. Dielectric Elastomer Actuators

DEAs are mechanomorphs that switch their shapes when an electric field is applied between the two sides of the sheet. The electric field induces mechanical contraction in the direction of the field and mechanical expansion in the perpendicular plane as elastomers are incompressible. When it is laminated to a passive layer without any mechanical response to the external field, such material can bend because of different residual strains upon electric current. The principle of this morphing mechanism is displayed in **Figure 12**A. To be able to obtain a proper shape-change, the elastomer layer should be as soft as possible and with a high electrical permittivity.

Very often, such actuators are processed to be bended in their initial shape and the folded shape is then modified by the electric field. For this initial bending, the elastomer layer is prestretched and glued to a flexible nonresponsive layer at rest. Thus, after mechanical release, the stretched elastomer layer constrains the other one in compression creating an out-of-plane buckling responsible for folding. Applying a voltage will shift the energy balance toward another minimum corresponding to another shape. The shape morphing will then depend on the applied voltage but also on the initial deformation.[132] Up to now, the most commonly used elastomer material is acrylic foam adhesive (VHB adhesive from 3 M). As it is an adhesive itself, it is very convenient for lamination. Nevertheless, high voltages are still

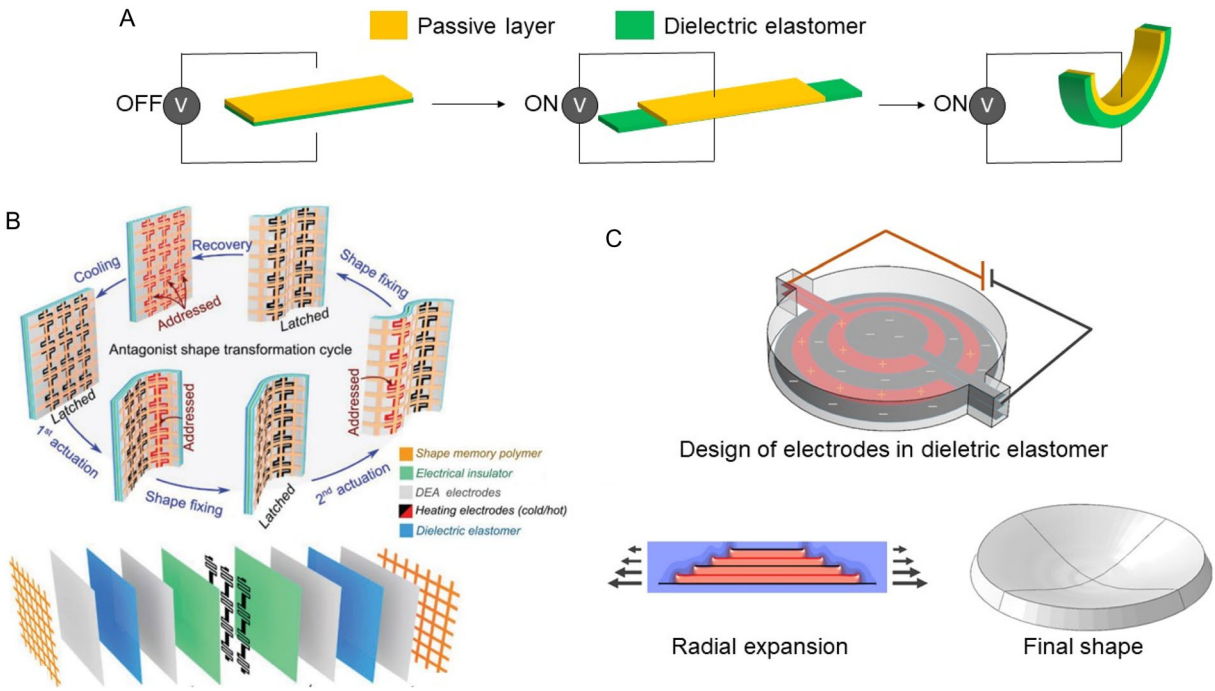

Figure 12. A) Schematic principle of dielectric elastomer actuators, B) sequential shape locking and shape reversibility of DEAs [Reproduced with permission.[139] Copyright 2024, Wiley], C) patterned electrodes to get a dome shape [Reproduced under the terms of the CC-BY 4.0 license.[141]].

required for actuation. For instance, when an acrylic layer is attached to a PET layer, the service voltage is around 3.4 kV.[133] Anyway, in each material, there is a structural saturation voltage that implements a safety limit.

Because DEAs intrinsically need soft materials to morph, for some applications, these actuators might be too soft and thus are often reinforced. First, the prestretching often used in the process is in fact a strategy to stiffen the material, as it is already in tension. Second, stiff fibers can be inserted in the layers. These fibers not only reinforce the actuator but are also responsible for controlling the direction of actuation. It was interestingly showed that with one central fiber, the ratio of Young moduli between the fiber and the elastomer matrix will control the side of folding.[134] A complex fan shape was even obtained with vinyl fibers in an acrylic elastomer. In this case, the prestretching was not even necessary then not implemented in the process. Counterbalancing the need of a prestretching step can also expand the lifetime of the actuator because highly prestretched elastomers can more easily creep or tear, inducing performance loss. Another study used glass fibers with optimized fiber spacing and orientation to obtain twisting in addition to bending.[135] Third, some examples demonstrated a reinforcement with the use of an external ladder frame.[136,137] These architectures were responsible for the enhancement of the force distribution and an increase of up to 40 times in the tension-induced moment.

In the DEAs field, there are mainly three different class of accessible elastomers: acrylic adhesives, polysiloxanes for their well-known elasticities and relatively easy functionalization, and polyurethanes. Kyung's group reviewed in 2020 the main applications of DEAs giving an interesting overview on the recent achievements in artificial muscles, grippers, walkers, or adaptive lenses.[138] We will rather focus here on the comparison with the other morphing systems, highlighting the remaining challenges presented in the review and stressing the most recent studies tackling them.

As with actuators described in previous sections, shape locking to stop the external trigger is a recent concern, and of particular interest to reduce energy consumption, as the external power supply can be stopped after morphing. Shape locking was achieved by laminating a thermoresponsive layer over the voltage-responsive elastomer.[139] When this added layer is heated, it becomes soft enough to be actuated by the voltage actuation of the DEAs, but it is too stiff to enable the DEAs to move when cooled down. Thus, by playing on the temperature with a layer of affordable T_g, shape locking is quite easily imparted. Nevertheless, shape reversibility is still accessible upon a second trigger. In addition, the softening upon heating could be localized such that sequential foldings could be obtained (Figure 12B). The direction of folding could even be tuned by the direction of the softened part.

More complex deformations than bending are also foreseen. They can be achieved by designing complex structures such as tensegrity structures that are architecture structures with rods and cables self-supported via an equilibrium between tension and compression forces.[140] Moreover, it was also obtained by patterning the elastomer and/or electrodes.[141,142] First, the electrodes were patterned as concentric rings leading to radial differential expansion of the underlying elastomer and a final dome shape (Figure 12C).[141] Second, the electrode can be post-process patterned by laser etching without damaging the elastomer underneath.[142] Interestingly, this could be implemented to create an anisotropy in the mechanical behavior of localized domains of the elastomer. Such laser processing has an optical resolution of 20 μm opening new opportunities toward miniaturized DEAs.

Up to now, safety remains the main limit of these DEAs. There are two possibilities to make them safer: insulate the electrodes to avoid contact with the exterior and work on the materials to lower the required voltages. An underwater swimmer was insulated by sandwiching two electrodes between three layers of elastomer.[143] This can be responsible for smaller morphing but in this example, the specific design creating an indirect bending via an alternate lever effect led to enough deformations to reach a speed of 0.9 mm s^{-1} in water. Even if polysiloxanes were not the most used elastomers, notably because of their lower electrical permittivity and lower electrical breakdown at 1400–2000 V compared to acrylic elastomers, they present the main advantage to be able to morph at higher frequencies, as rapid and complete shape reversibility was obtained. So, those are still preferred for some applications. They were recently functionalized with polar side groups on the main chain to tune their permittivity.[144,145] When the chain ends remain active, self-healing was even possible after electrical breakdown for instance.[145] However, in this case, the recycling ability is finite because electric breakdown induces local permanent defects after heat shock, inducing performance loss.

DEAs offer a different trigger from mechanical actuation, but the material still needs to be in contact with the trigger source, and the morphing cannot be localized. Therefore, mechanomorphs with a remote trigger were investigated thanks to specific materials: the liquid crystal elastomers.

5.3. Liquid Crystal Elastomers

Liquid crystal elastomers (LCEs) are mechanomorphs that shapes change when the liquid crystals in the chains, called mesogens, locally reorient or lose their order upon external triggering, causing local mechanical expansions or contractions. These LCEs can respond to heat, light, or even humidity. In contrast to hygromorphs, it is not a differential swelling, but differential expansions due to an indirect trigger from water molecules on the mesogens. The first reason for LCEs morphing is a mesoscopic loss of ordering caused by temperature or NIR light with photothermal effect where it goes through the nematic-isotropic phase transition temperature (T_{NI}). The second reason for LCEs morphing is at the molecular level with a trans-cis isomerization of the mesogens caused by UV light. Light- or humidity-responsive materials can be monolayer systems because the trigger can be easily localized in-plane but also in depth.

LCEs can morph by crossing the T_{NI}. Thus, to obtain a nematic phase, the mesogens must be oriented in an anisotropic pattern during the processing step. Upon heating above T_{NI}, the orientation is lost causing a gradient of residual strains due to differential expansions along the anisotropic thickness. One possibility to orient such crystals during processing is to use a filling-chamber with micro-channels patterned in the internal surfaces.[146] To create anisotropy, it is possible to tilt the upper

pattern compared to the bottom one. The channel depth and width must be carefully controlled to be large enough for orienting but small enough to continuously implement a direction. Compared to DEAs, LCEs are intrinsically stiffer and can weight greater lifts. One example showed that it was able to lift 784 times its own weight. In this strategy, fast gelation is a key for fixing the molecular order. Methacrylates are thoroughly used for the appropriate kinetics of free-radical cross-linking but require an oxygen-free atmosphere.[147] The cross-linking by thiol-ene reaction of dithiols with acrylates is advantageously used in presence of oxygen. Moreover, tuning of the T_{NI} is possible by mixing and controlling the ratio of two different commercially available liquid crystals, namely RM82 and RM257.[147]

In the case of an indirect actuation, thanks to the photothermal effect of NIR on convertors, the anisotropy can be obtained not by patterning the mesogens but controlling the distribution of the photo-thermal convertors such as Au nanoparticles.[148] In this study, the processed LCE was swollen with a gold salt $HAuCl_4$ which was then photo-reduced into Au nanoparticles. Thus, the anisotropy was created easily with photomasks to locally reduce the gold salt or not which can then be rinsed out of the matrix. Then, as it simply relies on masks, it opens up new possibilities to obtain an anisotropic response for morphing.

NIR photothermal remote actuation was advantageously used in complex systems toward applications. Indeed, one LCE layer was combined with a photochromic layer in a bilayer camouflage and morphing system.[149] This material can then change color, from light blue to red in function of the opened/closed isomers fluorescing or not. Thus, it could crawl on a surface which was painted in blue and red and could change color to adapt to the surface. Another example was inspired by the flytrap taking advantage of the reflectance of light coming from the LCE on an approaching object (**Figure 13**A).[150] Light was then going back to the surface of the LCE triggering the switch entrapping the object in only 200 ms.

Another possible trigger for LCEs is UV light able to photocatalyze a *trans*-cis isomerization, this molecular switch leads to macroscopic morphing. Azobenzene presents the advantage to have a reversible trans-cis isomerization.[151,152] In contrast to nematic-isotropic transitions, isomerization has to be triggered again to retrieve the initial shape meaning that shape locking occurs. Indeed, after removal of UV, the isomerization remains and the morphed shape is locked. Irradiation with visible light reversing the isomerization triggers switching back to the initial shape. It is worth noting that azobenze mesogens remain liquid crystals thus can still be triggered with temperature or NIR light via T_{NI}. These are thus involved in multiresponsive mechanomorphs illustrated in Figure 13B. Moreover, Zhao's group interestingly showed that embedding Au nanorods for a photothermal effect enhanced the UV response of the system.[151]

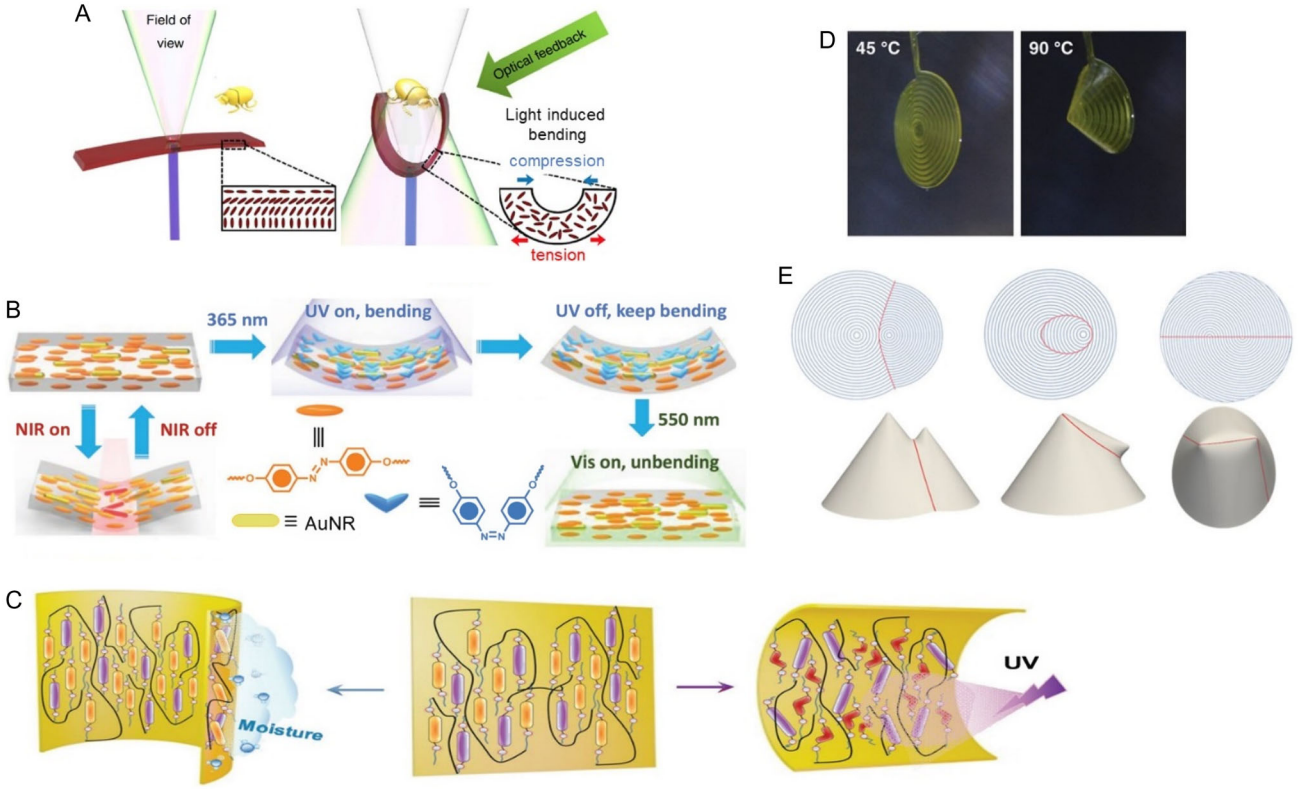

Figure 13. A) Light-induced nematic-isotropic transition in a biomimetic flytrap triggered by an optical reflexion from an approaching object [Reproduced under the terms of the CC-BY 4.0 license.[150]], B) multiresponsive LCE with azobenzene [Reproduced with permission.[151] Copyright 2024, Wiley], C) moisture and UV responsive [Reproduced with permission.[152] Copyright 2024, Wiley], D) 3D-printed LCE concentric rings which transition is triggered by temperature [Reproduced with permission.[155] Copyright 2024, Wiley], E) stitching separately fabricated patterns to create more complex shapes [Reproduced under the terms of the CC-BY 4.0 license.[157] Copyright 2024, The Authors. Published by RSC].

Another example proved this multiresponsivity with UV and humidity.[152] Interestingly, in response to moisture, the LCE bends in opposite to the source and parallel to the liquid crystal alignment, and in response to UV, it bends toward the source and perpendicular to the liquid crystal alignment (Figure 13C). To the best of our knowledge, there is no discussion on the cyclability of such chemical mechanisms to go back and forth between the shape and should be more detailed in the future.

In addition to shape locking, shape-reprogramming was successfully managed by using a liquid crystal vitrimer.[153] Upon transesterifications catalyzed by triazabicyclodecene, one morphed shape could be reset as the initial shape after heating for chain rearrangement to relieve the stress stored in the deformation.

Finally, complex shapes were obtained by orienting the crystals in micro-domains with a polarized light, by shear alignment during 3D printing, or by stitching together LCE parts fabricated separately. Azobenzene was successfully oriented along the direction of a polarized laser at 445 nm. White's group managed to implement 226 distinct directions in 21 350 micro-domains.[154] They obtained dome shapes after self-morphing by encoding a pattern of micro-domains which orientation varies in-plane around a central point. Here again, like for in-plane cross-linking gradient in hygromorphs, the deformation can be upward or downward and if multiple patterns were encoded side by side, several shapes are obtained.

3D printing allows LCE chains alignment along the path of the needle by extrusion-deposition shear forces.[155] By printing concentric rings, cone shapes are obtained after morphing (Figure 13D). In this process, the nozzle diameter is key. Indeed, reducing the nozzle diameter increases the resolution but also increases the required forces for extrusion which impacts the further shape-transition.[156] By varying the width of the concentric rings, it was possible to reach a dome 10 times higher than the sheet thickness. Recently, complex shapes were also created by stitching together relatively simple patterns acting as building blocks.[157] To keep a continuous deformation, only a few possibilities for stitching two patterns together exist, according to the printing lines, as displayed in Figure 13E. When it is not compatible, the materials will suffer more easily from failures upon deformations.

A last recent example of mechanomorphs triggered by heat is the elegant combination of an off-centered core fiber of a shape-memory polymer inside a shell of an elastic one. This way, heat reversibly modify the strain difference between the core and the shell and make the composite coil and uncoil.[158]

LCEs being multiresponsive, they probably inspired other triggers for mechanomorphs. Indeed, because mechanomorphs rely on a simple principle, multiple triggers are accessible, like visible light but also enzymes for differential degradation and DNA linkers for interparticle shrinking distance.

5.4. Visible Light, Enzymes, and DNA Triggers

Besides temperature or light, mechanomorphs can be triggered by enzymes as well as, in a very recent study, DNA linkages.

The most direct strategy for thermal trigger is building the bilayer with two materials of distinct coefficients of thermal expansion (CTE). Even though it was the first strategy for actuators just like the bimetallic strip of Timoshenko, it is not exploited anymore, especially in soft materials. One reason might be that the induced gradient in expansion will not be as steep as it can be with other strategies, limiting the extent of the shape-change. Nevertheless, some studies showed not only enhanced morphing but also indirect actuation using a bilayer with different CTEs. For example, it was shown that a bilayer of poly(ethylene) (PE) and a U-shaped graphite electrode could bend with a curvature of at least 140° through electrothermal heating at 1.5 V.[159]

Another strategy for remote trigger of mechanomorphs is to locally release some stored mechanical stress, simply by local heating of a prestressed sheet to soften and relax only the local hinges above T_g. Localized heating is most often achieved by a photo-thermal convertor providing light trigger. It has been implemented in an innovative way by adding desktop inks of different colors on some hinges.[160] These were selectively light triggered by choosing the color of LEDs giving the maximum absorbance for each colored hinge as shown in **Figure 14**A. Sequential folding was achieved by illuminating each hinge that conducted to localized shrinkage on the targeted side. This partial photo-induced stress release could also be made via photochemical chain cleavage and rearrangement.[161] This strategy is very helpful if sequential morphing is foreseen, but reversibility is not accessible, and shape reprogramming would depend on ink removal but was not discussed.

Besides, the gradient in residual strains can be obtained by differential degradation of the materials. Gracias' group took advantage of the different enzymatic degradation rates of polypeptides and polysaccharides (Figure 14B).[162] For instance, gelatin is degraded in 30 min or over one week depending on the enzyme. This offers the possibility for autonomous sensing in response to a disease marker such as proteases in cancer. It is also possible to make the sensor more specific by delaying the enzymatic degradation using enzyme inhibitors. With this kind of trigger, it could be more straightforward, compared to hygromorphs and magnetomorphs, to reduce the size of the designed objects. For medical applications, but not only, micro morphing objects could become valuable.

Toward this end, Park's group reported on a material able to locally shrink or expand by playing on the extent of linking between DNA-functionalized Au nanospheres and nanorods.[163] Two neighbor particles interact by DNA chain linkage, this interaction being reinforced by adding a third bridging sequence complementary to both of the others, this leads to the decrease of interparticle distance and local shrinkage (Figure 14C). This contraction is released by adding a fourth sequence interacting more favorably to the bridging DNA strand. With this trigger, the dimension of local shape changing can be considerably reduced toward micro- or nanomaterials. One could imagine an application as a nanosensor to specific DNA sequences.

In conclusion, these mechanomorphs present the main advantage to have the largest variety of the accessible materials because they must only differ in their mechanical behavior. In addition, complex systems with shape locking and shape-reprogramming are easy to get. Up to now, the main limit of this

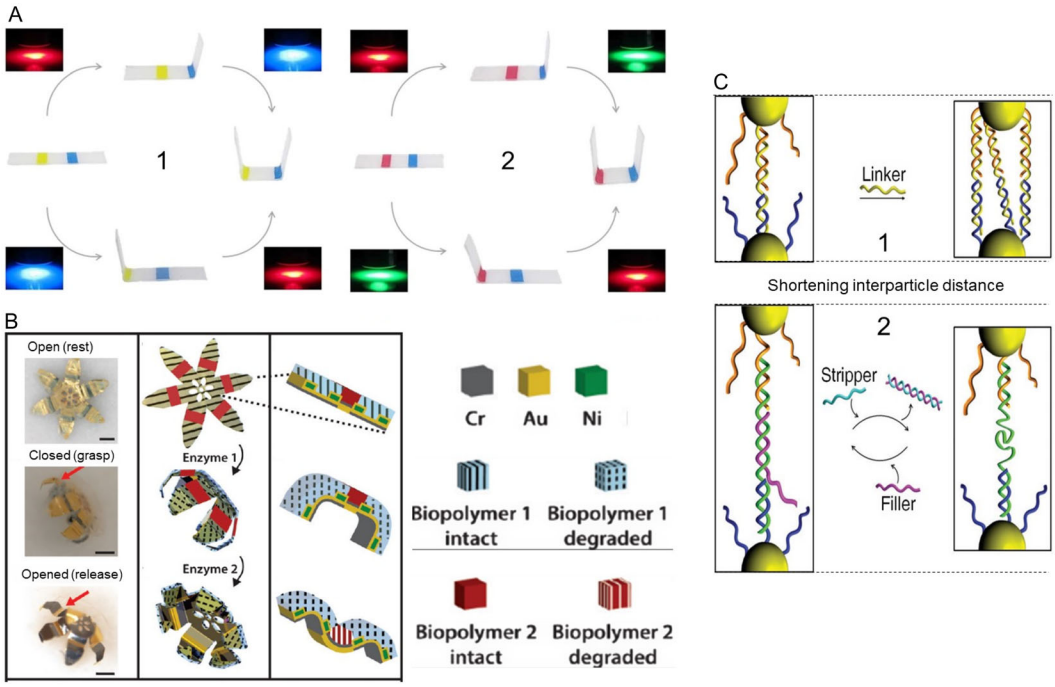

Figure 14. A) Sequential folding with visible light LEDs on desktop ink printed hinges [Reproduced under the terms of the CC-BY 4.0 license.[160]], B) differential degradation kinetics of biopolymers leading to difference in mechanical properties and morphing [Adapted with permission.[162] Copyright 2024, American Chemical Society], C) DNA chains as a reversible tool to locally modify the interparticle distance [Reproduced with permission.[163] Copyright 2024, Wiley].

field remains maybe the narrow diversity of morphed shapes that were reported. Therefore, we believe that this is the major foreseen innovation. Moreover, we believe that discussion about cyclability and performance loss should be more regularly implemented. Finally, the lately described systems could inspire new substrategies for mechanomorphs, opening ways for the creation of miniaturized devices that respond autonomously to specific biochemicals or disease markers.

6. Baromorphs and Cellularomorphs

A few other strategies are not falling into the previously described families of hygromorphs, magnetomorphs, and mechanomorphs. Up to now, they are also less referenced. Among these, we will illustrate baromorphs and cellularomorphs.

6.1. Baromorphs

Potentially bioinspired from depressurized bladderworts, baromorphs are actuators that adapt their shapes upon a positive or negative pressure. Essentially, a network of air channels, connected to a compressed air source or vacuum pump, is embedded in between two elastomer layers. Morphing is then obtained upon inflation when there is an anisotropy, which can be created out-of-plane by either two different stiffnesses for the two elastomer layers, or thinner walls on one side. The principle is presented in **Figure 15**A. It can also be obtained in-plane by welds separating isotropic air expanded channels (Figure 15B). Slightly different, extendable channels can be inserted in a shell of a restrictive material but incised to let the expansion in some points. Finally, vacuum can be used for locomotion via a lever effect.

Pneumatic networks, called PneuNets by their authors back in 2011, use two elastomers of different stiffness with air channels in between.[164,165] Upon inflating ($P < 30$ kPa), the stiffer elastomer layer restricts expansion on its side, while the softer elastomer layer enables air blowing on the other side. These air channels are created by laminating on the flat passive layer, the patterned active layer with its structures facing the passive layer (Figure 15C). The morphing depends on the geometry and occurrence of airways and the applied pressure. These baromorphs present the advantage to be under tension while inflated which brings rigidity. The absence of joints makes them capable of easily grasping irregular objects. These make them good candidates for gripper applications, and a textured passive layer was even available to enhance the gripping ability.[165] Complexed shapes inspired by *Acetubalaria* have been obtained.[164]

In these systems, shape locking was readily achieved by closing the connection to the compressor, but it is not permanent due to gas permeability. The system was completely deflated after 60 min.[165] Later, this strategy has been used to design a walker composed of four legs and one body fed by different air sources independently activated.[166] By sequential activations, it is able to walk at a speed of up to 24 m h^{-1}, so as to go underneath obstacles (Figure 15D). Such PneuNets can also be designed with a unique material but with thinner walls between the air channel

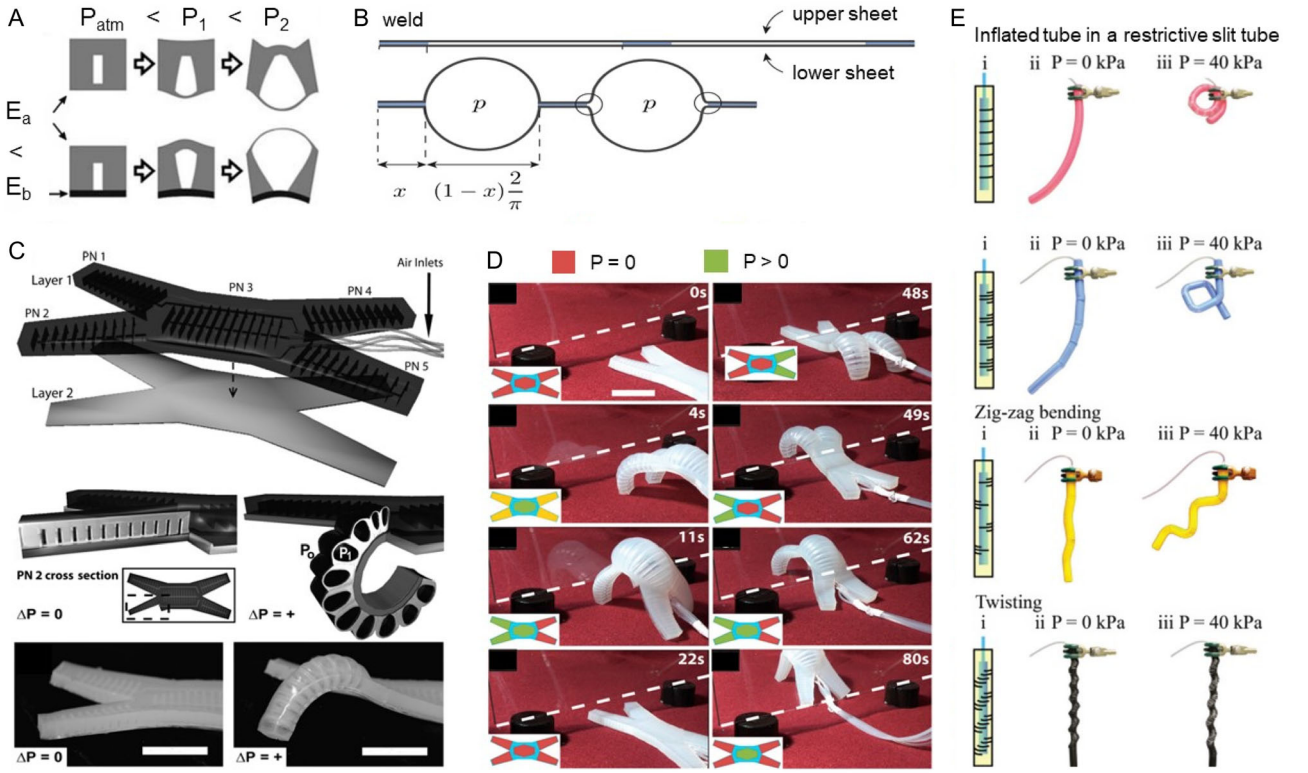

Figure 15. A) Principle of baromorph with a unique material or two different layers [Reproduced with permission.[165] Copyright 2024, Wiley], B) principle of in-plane baromorphs [Reproduced with permission.[168] Copyright 2024, RSC], C) PneuNets bilayer with air channels (scale bar: 3 cm) [Reproduced with permission.[166] Copyright 2024, National Academy of Sciences], D) PneuNet multiarm robot sequentially folded to go underneath an obstacle (scale bar: 4 cm) [Reproduced with permission.[166] Copyright 2024, National Academy of Sciences], E) several slit patterns on a restrictive tube for several morphing [Reproduced with permission.[170] Copyright 2024, Wiley].

and the exterior only on one side to favorize air blowing towards this layer which flexural rigidity decreases.[165] For monomaterials, one layer can be prestretched to achieve bending. Depending on the ratio of heights, the initial curve can be oriented in two directions, but after inflating the curve always presents the blown layer on the outside. This principle was turned into advantage to enable a curve on one side at rest and a curve in the other direction after inflating.[167] This study also proved the locomotion ability by creating a gradient of height for the parallel air channels from head to tail, which can be amplified by adding an extra weight in the head of the self-moving object.

Another strategy to create baromorphs is to impregnate poly(amide) patterns that are hermetic to air in thermoplastic poly(urethanes) (TPU).[168,169] It was specially designed to create in-plane anisotropy between restrictive welds and isotropically blown air channels. They were able to obtain complex patterns such as a dodecahedron from a planar sheet or shapes made of mountains and valleys. This strategy enables the mechanical strengthening of the actuator.

Baromorphs have also been designed with a pressure responsive elastomer tube inserted in a restrictive bigger tube.[170] The external stiffer tube can control the shape change by a pattern of cuts. The angles, positions, periodicities, and lengths of the slits control the bending or twisting of the whole structure upon inflating the internal tube as shown in Figure 15E. When several tubes connected to independent air pumps are added in the external tube, sequential and different directions of self-folding are obtained. Thus, a multitask actuator was designed and able to lift and screw a bulb.

Finally, vacuum was advantageously used to morph via the collapse of anisotropically distributed holes.[171] This creates the rotation of the elastomer part situated in between the holes and can be used for locomotion via the lever effect like oars of a boat. The main advantage of the vacuum compared to compressed air is that the actuator volume does not increase upon actuation.

In general, the advantages of the baromorphs compared to other morphing systems are their easy design and easy access to actuation source, as well as to lightweight, simple, and environmentally benign materials. With this strategy, it is easy to have fast and complete reversibility in between the accessible shapes, and it seems safe to consider that it should retain similar performance for a lot of cycles. In the opposite, the main disadvantage is that is has to be permanently connected to the source with tubing, even untethered systems, and could limit the possible applications as a pump or air supplier must always be carried on.

6.2. Cellularomorphs

Going even further toward safe processes, in the line of using air at relatively low pressures as a trigger, recent reports used the

inherent contraction of cells to impart morphing. Cellularomorphs change their shapes due the tensile force exerted by cells, either embedded in collagen gels or deposited on top of cell-adhesive surfaces. In vivo, cells fold the extracellular matrix (ECM) when they are migrating, proliferating, or differentiating. Inspired by these, synthetic cell-loaded collagen gels were proven to modify their shapes. Interestingly, it is another strategy to induce morphing at the microscale. Herein, anisotropy is created by the simultaneous cell sedimentation and gelation.[172] The morphing depends on the nature and density of the cells and on the collagen concentration that impacts the structure of the fibrils. Then, the deformed shape itself also induces fibril orientation and is responsible for a topographical smoothing.[173] Qin's group took advantage of these parameters, especially differential cell tensile force (CTF) with different cells embedded in two layers (**Figure 16**A).[174] Moreover, cell contraction inhibitors can be locally implemented to regulate the CTF and induce morphing as a dome via an in-plane gradient (Figure 16B). As it is difficult to control the cell sedimentation upon gelation, the distribution is random, but structuring the backside with a pattern of ridges enables to govern the direction of folding.[174]

Another category of cellularomorphs add the cells on top of the material instead of inside the matrix. This opens up new possibilities for accessible materials for the substrates, it only requires to be cell adhesive, but this can be easily tuned with coatings such as fibronectin. Cells contracting on one side at the junction between microplates were able to fold the structures.[175] Without connection between plates, complete folding is reached. With a joint, two plates side to side can collide, then the angle (θ) is limited and can be calculated in function of the geometric parameters as $\theta = \frac{2w}{r+t}$ with w is the width of the joint, t is the thickness of the joint, and r is the thickness of the plate. Complex 3D objects such as dodecahedron and tubes were obtained and are displayed in Figure 16C.

Up to now, the main limit of these cellularomorphs is the actuation speed. For some applications, it could be interesting to have a sequential morphing, for others it would require faster actuation. Khademhosseini's group smartly made faster the folding by embedding a layer of Au microelectrodes underneath to stimulate the cells.[176] Beating was even possible after reinforcing by laminating PEG to increase the stability of the structure. The frequency could not overcome 0.5 Hz to allow a complete recovery before another contraction. In this example, cardiomyocytes were used and aligned along a pattern to bring anisotropy.

These cellularomorphs could be very useful in the near future for the development of smart biomedical devices, since exploiting cells is an advantage for in vivo autonomous morphing devices. In addition, a variety of cells compatible hydrogels is already identified from tissue engineering research field, allowing to investigate the effect of different cells, cell density, and ageing on cellularomorphs performances. However, this strategy might be limited to micro-objects as it is most probable that for the CTF to induce morphing, the substrate should have dimensions close to the ones of cells. Nevertheless, for medical applications, micro-objects can already be very valuable. Bringing together researchers in both materials and medical fields would insure fast development of cellularmorphs and emergence of cells controlled biomedical devices. Finding a way to increase the dimensions of the morphing systems with this strategy could also be an important breakthrough. The cellularomorphs are also intrinsically irreversible, and strategies to enable coming back to

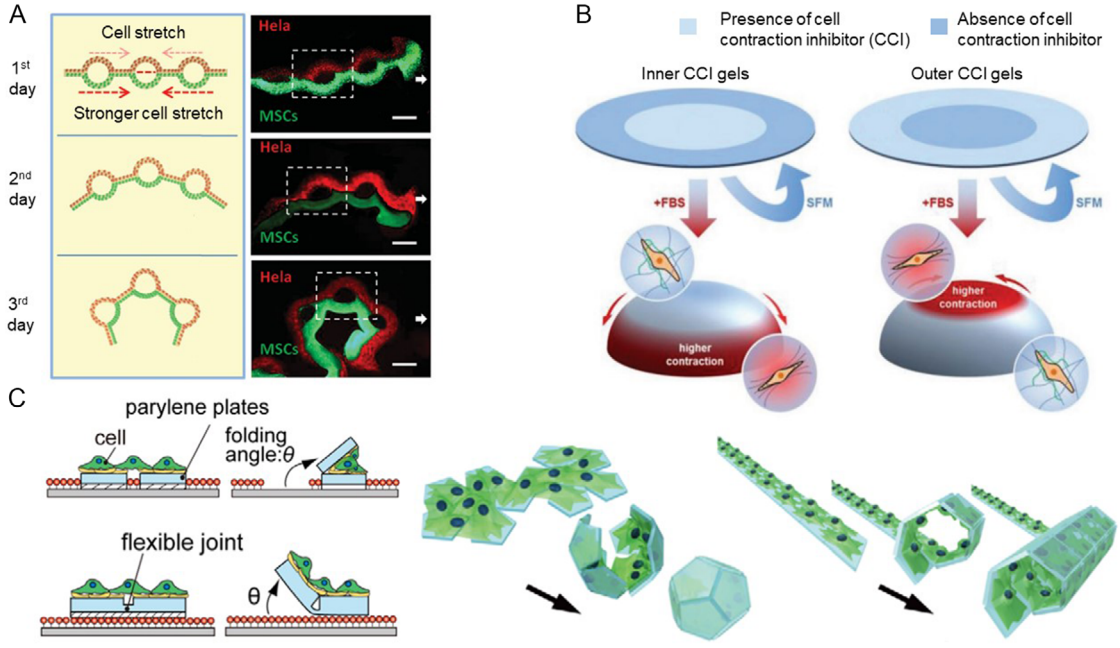

Figure 16. A) Differential compression on a bilayer due to different cells on each layer [Reproduced with permission.[174] Copyright 2024, Wiley], B) dome shapes obtained with the local deposition of a cell contraction inhibitor (CCI) in a fetal bovine serum (FBS), while no folding was obtained in serum-free medium (SFM) [Reproduced with permission.[173] Copyright 2024, Wiley], C) cell contraction imparting folding on parts or jointed substrates giving dodecahedron or tubes [Reproduced under the terms of the CC-BY 4.0 license.[175]].

its initial position, like adding cells on the other side, should be investigated in the future.

7. Conclusion and Perspectives

Plants have evolved through the centuries by optimizing their growth, feeding, and seed dispersal to improve their survival. Notably, several plants have developed the ability to change their shapes in order to fulfil one of the requirements for the sustainability of the species. Specifically analyzing the mechanisms underlying these evolutions and their potential triggers inspired humans to develop new synthetic shape-adaptable systems in a biomimetic way. For instance, pinecone inspired hygromorphs, morphing upon a differential swelling. Cyclamen had first optimized differential growth, similarly to mechanomorphs, shape-changing upon differential elongations. Flax seeds might have inspired magnetomorphs, where a patterned internal magnetization constrains the matrix to reach another shape. Baromorphs morphing thanks to air blown in patterned channels remind of carnivorous bladderworts. Each class of synthetic morphing materials presents several advantages.

Hygromorphs, bio-inspired by the most common strategy in the plant kingdom, are by far the most reported shape-adaptable materials. This gives rise to a large panel of triggers thanks to responsive hydrogels and robust design processes. The most recent discoveries concern the feasibility of imparting an in-plane cross-linking gradient or post-modify the crosslinking density very locally. Nevertheless, hygromorphs must be kept in specific environments and few locking strategies were investigated.

Additionally, magnetomorphs were developed. They possess the advantage that magnetism is probably the safest trigger, notably for in vivo applications as it does not affect body tissues. This is without doubt the morphing strategy that led to the most complex shapes thanks to the ability to print micro-domains. Nevertheless, magnetic particles must be used as fillers which might bring toxicity, and thus could be an issue for biomedical uses.

Mechanomorphs rely on the most simple and straightforward mechanism of action. This enabled this class of materials to present the widest possibilities for actuation, ranging from classical heat or light to mechanical, enzymatic and DNA-linkage triggers. This is also the simplest strategy to obtain shape locking and shape reprogramming with shape-memory composites for instance. Other categories of elastomers, such as biodegradable elastomers, should still be developed and applied to mechanomorphs exhibiting these very important features that enable to stop the actuation once the movement is obtained and eventually reset it at will.

Baromorphs, operated by compressed air, benefit from safe, fast, and reversible actuation. Indeed, air can be very rapidly blown in the channels and as rapidly removed. Quite recent, this strategy holds nevertheless a strong potential, notably for sequential activation of robots.

More generally, whatever the actuation mechanism, shape-changing materials are particularly promising and thus the focus of investigations was recently turned toward biomedical applications. The pioneer works on cellularomorphs and enzyme-triggered mechanomorphs have paved the way for the design of devices morphing in vivo by autonomous actuation in response to specific biomarkers. To push further, safer processes and biocompatible platforms have to be developed synergistically. In our opinion, the development and use of degradable materials dedicated to these smart devices is still understudied, where biodegradable morphing devices would represent a breakthrough in the medical field by removing some technological barriers. For instance, implants with shape adaptability are the gold standard for noninvasive surgeries, as it could deploy and adopt the specific geometry only once onsite. For applications where the implant has a temporary role, the selection of biocompatible degradable materials to build this implant might be particularly attractive. Indeed, degradation products excreted by the body or bioabsorbed will prevent needless accumulation in the body. Development of degradable shape-changing devices, today disregarded, could thus lead to important breakthroughs.[177] The development of materials offering tailor-made biodegradation therefore seems crucial for future progress in this field.

A few key points can be highlighted for the future development of this field. There are many opportunities for new materials to overcome certain technological hurdles, as they are currently limited to a few. Porous materials such as foams have great potential for lightweight smart devices and have not yet been studied too much.[178] Modeling remains very important for translating observations in nature into morphing systems. These models are extremely useful for assessing cyclability and loss of performance during aging, which are often difficult to measure.

Acknowledgements

O.R. thanks the «Fonds de la Recherche pour l'Industrie et l'Agriculture» (FRIA) for Ph.D. grant.

Conflict of Interest

The authors declare no conflict of interest.

Author Contributions

Oscar Rabaux: Conceptualization (lead); Writing—original draft (lead). **Christine Jérôme**: Conceptualization (supporting); Funding acquisition (lead); Resources (lead); Writing—review & editing (lead).

Keywords

bioinspiration, smart morphing, soft system

Received: April 26, 2024
Revised: July 4, 2024
Published online: August 18, 2024

[1] L. Guiducci, J. W. C. Dunlop, P. Fratzl, *On Folding: Towards a New Field of Interdisciplinary Research*, Transcript, Verlag, Bielefeld, Germany **2016**.
[2] S. Timoshenko, *J. Opt. Soc. Am.* **1925**, *11*, 233.
[3] D. L. De Voe, A. P. Pisano, *J. Microelectromech. Syst.* **1997**, *6*, 266.

[4] F. L. Bargardi, H. Le Ferrand, R. Libanori, A. R. Studard, *Nat. Commun.* **2016**, *7*, 13912.
[5] Y. Zhang, H. Le Ferrand, *Biomimetics* **2022**, *7*, 13.
[6] S. Li, K. W. Wang, *J. R. Soc., Interface* **2015**, *12*, 20150639.
[7] J. Liu, Y. Gao, Y.-J. Lee, S. Yang, *Trends Chem.* **2020**, *2*, 107.
[8] L. Hu, Y. Wan, Q. Zhang, M. J. Serpe, *Adv. Funct. Mater.* **2020**, *30*, 1903471.
[9] J. Dumais, Y. Forterre, *Annu. Rev. Fluid Mech.* **2012**, *44*, 453.
[10] S. Poppinga, C. Zollfrank, O. Prucker, J. Rühe, A. Menges, T. Cheng, T. Speck, *Adv. Mater.* **2018**, *30*, 1703653.
[11] Y. Chi, Y. Li, Y. Zhao, Y. Hong, Y. Tang, J. Yin, *Adv. Mater.* **2022**, *34*, 2110384.
[12] R. Elbaum, Y. Abraham, *Plant Sci.* **2014**, *223*, 124.
[13] C. Dawson, J. F. V. Vincent, A.-M. Rocca, *Nature* **1997**, *390*, 668.
[14] H. Bae, J. Kim, *Plants* **2020**, *9*, 1343.
[15] E. Reyssat, L. Mahadevan, *J. R. Soc., Interface* **2009**, *6*, 951.
[16] I. Burgert, P. Fratzl, *Philos. Trans. R. Soc., A* **2009**, *367*, 1541.
[17] R. Elbaum, S. Gorb, P. Fratzl, *J. Struct. Biol.* **2008**, *164*, 101.
[18] S. Armon, E. Efrati, R. Kupferman, E. Sharon, *Science* **2011**, *333*, 1726.
[19] R. M. Jones, *Mechanics of Composite Materials*, CRC Press, Boca Raton, FL **1998**.
[20] M. J. Harrington, K. Razghandi, F. Ditsch, L. Guiducci, M. Rueggeberg, J. W. C. Dunlop, P. Fratzl, C. Neinhuis, I. Burgert, *Nat. Commun.* **2011**, *2*, 337.
[21] S. Poppinga, M. Joyeux, *Phys. Rev. E* **2011**, *84*, 041928.
[22] V. S. Markin, A. G. Volkov, E. Jovanov, *Plant Signaling Behav.* **2008**, *3*, 778.
[23] Y. Forterre, J. M. Skotheim, J. Dumais, L. Mahadevan, *Nature* **2005**, *433*, 421.
[24] I. R. Macdonald, D. C. Gordon, J. W. Hart, *Plant, Cell Environ.* **1987**, *10*, 613.
[25] W. R. Briggs, *Plant Sci.* **2016**, *353*, 541.
[26] J. P. Vandenbrink, E. A. Brown, S. L. Harmer, B. K. Blackman, *Plant Sci.* **2014**, *224*, 20.
[27] H. S. Atamian, N. M. Creux, E. A. Brown, A. G. Garner, B. K. Blackman, S. L. Harmer, *Plant Sci.* **2016**, *353*, 587.
[28] W. Shropshire Jr., *Phys. Rev.* **1963**, *43*, 38.
[29] P. Galland, A. Pazur, *J. Plant Res.* **2005**, *118*, 371.
[30] O. Vincent, C. Weißkopf, S. Poppinga, T. Masselter, T. Speck, M. Joyeux, C. Quilliet, P. Marmottant, *Proc. R. Soc. B* **2011**, *278*, 2909.
[31] P. H. Sydenham, G. P. Findlay, *Aust. J. Biol. Sci.* **1973**, *26*, 1115.
[32] O. A. Kuznetsov, K. H. Hasenstein, *Planta* **1996**, *198*, 87.
[33] M. Gajdardziska-Josifovska, R. G. McClean, M. A. Schofield, C. V. Sommer, W. F. Kean, *Eur. J. Mineral.* **2001**, *13*, 863.
[34] J. Shang, X. Le, J. Zhang, T. Chen, P. Theato, *Polym. Chem.* **2019**, *10*, 1036.
[35] L. Peng, J. Zhu, S. Agarwal, *Macromol. Rapid Commun.* **2017**, *38*, 1700034.
[36] S. Zakharchenko, E. Sperling, L. Ionov, *Biomacromolecules* **2011**, *12*, 2211.
[37] D. Lunni, M. Cianchetti, C. Filippeschi, E. Sinibaldi, B. Mazzolai, *Adv. Mater. Interfaces* **2020**, *7*, 1901310.
[38] J. Lou, Z. Liu, L. Yang, Y. Guo, D. Lei, Z. You, *Adv. Funct. Mater.* **2021**, *31*, 2008328.
[39] D. Correa, S. Poppinga, M. D. Mylo, A. S. Westermeier, B. Bruchmann, A. Menges, T. Speck, *Philos. Trans. R. Soc., A* **2019**, *378*, 20190445.
[40] A. Le Duigou, T. Fruleux, R. Matsuzaki, G. Chabaud, M. Ueda, M. Castro, *Mater. Des.* **2021**, *211*, 110158.
[41] T. Cheng, M. Thielen, S. Poppinga, Y. Tahouni, D. Wood, T. Steinberg, A. Menges, T. Speck, *Adv. Sci.* **2021**, *8*, 2100411.
[42] G. Stoychev, S. Zakharchenko, S. Turcaud, J. W. C. Dunlop, L. Ionov, *ACS Nano* **2012**, *6*, 3925.
[43] G. Stoychev, S. Turcaud, J. W. C. Dunlop, L. Ionov, *Adv. Funct. Mater.* **2013**, *23*, 2295.
[44] G. Stoychev, L. Guiducci, S. Turcaud, J. W. C. Dunlop, L. Ionov, *Adv. Funct. Mater.* **2016**, *26*, 7733.
[45] A. S. Gladman, E. A. Matsumoto, R. G. Nuzzo, L. Mahadevan, J. A. Lewis, *Nat. Mater.* **2016**, *15*, 413.
[46] T. Mora, A. Boudaoud, *Eur. Phys. J. E* **2006**, *20*, 119.
[47] K. Baek, J. H. Jeong, A. Shkumatov, R. Bashir, H. Kong, *Adv. Mater.* **2013**, *25*, 5568.
[48] M. Jamal, S. S. Kadam, R. Xiao, F. Jivan, T.-Z. Onn, R. Fernandes, T. D. Nguyen, D. H. Gracias, *Adv. Healthcare Mater.* **2013**, *2*, 1142.
[49] M. Pezzulla, G. P. Smith, P. Nardinocchi, D. P. Holmes, *Soft Matter* **2016**, *12*, 4435.
[50] J. Odent, S. Vanderstappen, A. Toncheva, E. Pichon, T. J. Wallin, K. Wang, R. F. Shepherd, P. Dubois, J.-M. Raquez, *J. Mater. Chem. A* **2019**, *7*, 15395.
[51] A. Kirillova, R. Maxson, G. Stoychev, C. T. Gomillion, L. Ionov, *Adv. Mater.* **2017**, *29*, 1703443.
[52] S. H. Kim, Y. B. Seo, Y. K. Yeon, Y. J. Lee, H. S. Park, M. T. Sultan, J. M. Lee, J. S. Lee, O. J. Lee, H. Hong, H. Lee, O. Ajiteru, Y. J. Suh, S.-H. Song, K.-H. Lee, C. H. Park, *Biomaterials* **2020**, *260*, 120281.
[53] C. Yao, Z. Liu, C. Yang, W. Wang, X.-J. Ju, R. Xie, L.-Y. Chu, *ACS Appl. Mater. Interfaces* **2016**, *8*, 21721.
[54] E. Palleau, D. Morales, M. D. Dickey, O. D. Velev, *Nat. Commun.* **2013**, *4*, 2257.
[55] A. B. Baker, D. F. Wass, R. S. Trask, *Sens. Actuators, B* **2018**, *254*, 519.
[56] A. B. Baker, D. F. Wass, R. S. Trask, *Smart Mater. Struct.* **2016**, *25*, 10LT02.
[57] D. Morales, I. Podolsky, R. W. Mailen, T. Shay, M. D. Dickey, O. D. Velev, *Micromachines* **2016**, *7*, 98.
[58] B. P. Lee, S. Konst, *Adv. Mater.* **2014**, *26*, 3415.
[59] B. P. Lee, A. Narkar, R. Wilharm, *Sens. Actuators, B* **2016**, *227*, 248.
[60] Z. Zheng, H. Wang, L. Dong, Q. Shi, J. Li, T. Sun, Q. Huang, T. Fukuda, *Nat. Commun.* **2021**, *12*, 411.
[61] C. N. Zhu, C. Y. Li, H. Wang, W. Hong, F. Huang, Q. Zheng, Z. L. Wu, *Adv. Mater.* **2021**, *33*, 202008057.
[62] J. Kim, J. A. Hanna, M. Byun, C. D. Santangelo, R. C. Hayward, *Science* **2012**, *335*, 1201.
[63] J.-H. Na, N. P. Bende, J. Bae, C. D. Santangelo, R. C. Hayward, *Soft Matter* **2016**, *12*, 4985.
[64] Y. Zhou, C. M. Duque, C. D. Santangelo, R. C. Hayward, *Adv. Funct. Mater.* **2019**, *29*, 1905273.
[65] L. Huang, R. Jiang, J. Wu, J. Song, H. Bai, B. Li, Q. Zhao, T. Xie, *Adv. Mater.* **2017**, *29*, 1605390.
[66] S. Zakharchenko, L. Ionov, *ACS Appl. Mater. Interfaces* **2015**, *7*, 12367.
[67] H. Arslan, A. Nojoomi, J. Jeon, K. Yum, *Adv. Sci.* **2019**, *6*, 1800703.
[68] I. Apsite, G. Stoychev, W. Zhang, D. Jehnichen, J. Xie, L. Ionov, *Biomacromolecules* **2017**, *18*, 3178.
[69] J. Wang, J. Wang, Z. Chen, S. Fang, Y. Zhu, R. H. Baughman, L. Jiang, *Chem. Mater.* **2017**, *29*, 9793.
[70] Y. Zhang, L. Ionov, *Langmuir* **2015**, *31*, 4552.
[71] A. Dallinger, P. Kindlhofer, F. Greco, A. M. Coclite, *ACS Appl. Polym. Mater.* **2021**, *3*, 1809.
[72] Y. Cheng, K. Ren, D. Yang, J. Wei, *Sens. Actuators, B* **2018**, *255*, 3117.
[73] T. S. Shim, S.-H. Kim, C.-J. Heo, H. C. Jeon, S. M. Yang, *Angew. Chem., Int. Ed.* **2012**, *51*, 1420.
[74] Z. J. Wang, C. N. Zhu, W. Hong, Z. L. Wu, Q. Zheng, *J. Mater. Chem. B* **2016**, *4*, 7075.
[75] C. Ma, T. Li, Q. Zhao, X. Yang, J. Wu, Y. Luo, T. Xie, *Adv. Mater.* **2014**, *26*, 5665.
[76] X. Li, X. Cai, Y. Gao, M. J. Serpe, *J. Mater. Chem. B* **2017**, *5*, 2804.
[77] K. Cho, D. Kang, H. Lee, W.-G. Koh, *Chem. Eng. J.* **2022**, *427*, 130879.

[78] L. Wang, Y. Jian, X. Le, W. Lu, C. Ma, J. Zhang, Y. Huang, C.-F. Huang, T. Chen, *Chem. Commun.* **2018**, *54*, 1229.
[79] C. Qian, Y. Li, C. Chen, L. Han, Q. Han, L. Liu, Z. Lu, *Chem. Eng. J.* **2023**, *454*, 140263.
[80] R. Luo, J. Wu, N.-D. Dinh, C.-H. Chen, *Adv. Funct. Mater.* **2015**, *25*, 7272.
[81] Y. Cheng, K. Ren, C. Huang, J. Wei, *Sens. Actuators, B* **2019**, *298*, 126908.
[82] S. Fusco, M. S. Sakar, S. Kennedy, C. Peters, R. Bottani, F. Starsich, A. Mao, G. A. Sotiriou, S. Pané, S. E. Pratsinis, D. Mooney, B. J. Nelson, *Adv. Mater.* **2014**, *26*, 952.
[83] S. Kodera, T. Watanabe, Y. Yokoyama, T. Hayakawa, *Micromachines* **2022**, *13*, 794.
[84] R. Yu, L. Zhu, Y. Xia, J. Liu, J. Liang, J. Xu, B. Wang, S. Wang, *Adv. Mater. Interfaces* **2022**, *9*, 2200401.
[85] G. Ge, Y.-Z. Zhang, W. Zhang, W. Yuan, J. K. El-Demellawi, P. Zhang, E. Di Fabrizio, X. Dong, H. N. Alshareef, *ACS Nano* **2021**, *15*, 2698.
[86] M. Kim, J. Choi, S. Y. Kim, *Mater. Today Chem.* **2022**, *26*, 101014.
[87] Y. Chandorkar, A. Castro Nava, S. Schweizerhof, M. Van Dongen, T. Haraszti, J. Köhler, H. Zhang, R. Windoffer, A. Mourran, M. Möller, L. De Laporte, *Nat. Commun.* **2019**, *10*, 4027.
[88] S. Maiz-Fernandez, L. Perez-Alvarez, I. Lopez de Munain-Arroniz, A. Zoco, A. C. Lopes, U. Silvan, D. Salazar, J. L. Vilas-Vilela, S. Lanceros-Mendez, *Int. J. Biol. Macromol.* **2022**, *219*, 374.
[89] T. Shiga, T. Kurauchi, *J. Appl. Polym. Sci.* **1990**, *39*, 2305.
[90] D. Han, C. Farino, C. Yang, T. Scott, D. Browe, W. Choi, J. W. Freeman, H. Lee, *ACS Appl. Mater. Interfaces* **2018**, *10*, 17512.
[91] Y. Wang, N. Alizadeh, M. Barde, M. L. Auad, B. S. Beckingham, *ACS Appl. Polym. Mater.* **2022**, *4*, 971.
[92] C. Yang, W. Wang, C. Yao, R. Xie, X.-J. Ju, Z. Liu, L.-Y. Chu, *Sci. Rep.* **2015**, *5*, 13622.
[93] Y. Li, Y. Sun, Y. Xiao, G. Gao, S. Liu, J. Zhang, J. Fu, *ACS Appl. Mater. Interfaces* **2016**, *8*, 26326.
[94] Y. Shin, M.-Y. Choi, J. Choi, J.-H. Na, S. Y. Kim, *ACS Appl. Mater. Interfaces* **2021**, *13*, 15633.
[95] L. Migliorini, T. Santaniello, Y. Yan, C. Lenardi, P. Milani, *Sens. Actuators, B* **2016**, *228*, 758.
[96] Q. Liu, Z. Dong, Z. Ding, Z. Hu, D. Yu, Y. Hu, N. Abidi, W. Li, *ACS Sustainable Chem. Eng.* **2018**, *6*, 7052.
[97] F. Wang, Q. Li, J.-O. Park, S. Zheng, E. Choi, *Adv. Funct. Mater.* **2021**, *31*, 2007749.
[98] K. Saeaeh, N. Thummarungsan, N. Paradee, P. Choeichom, K. Phasuksom, W. Lerdwijitjarud, A. Sirivat, *Eur. Polym. J.* **2019**, *120*, 109231.
[99] L. Reid, W. Y. Hamad, *ACS Appl. Polym. Mater.* **2022**, *4*, 598.
[100] A. Lopez-Diaz, A. Martin-Pacheco, A. M. Rodriguez, M. A. Herrero, A. S. Vazquez, E. Vazquez, *Avd. Funct. Mater.* **2020**, *30*, 2004417.
[101] I. Must, E. Sinibaldi, B. Mazzolai, *Nat. Commun.* **2019**, *10*, 344.
[102] L. Ionov, *Adv. Funct. Mater.* **2013**, *23*, 4555.
[103] M. Choi, B. Shin, H.-Y. Kim, *Soft Rob.* **2023**, *10*, 1171.
[104] V. Lutz-Bueno, S. Bolisetty, P. Azzari, S. Handschin, R. Mezzenga, *Adv. Mater.* **2020**, *32*, 2004941.
[105] H. Wang, Z. Zhu, H. Jin, R. Wei, L. Bi, W. Zhang, *J. Alloys Compd.* **2022**, *922*, 166219.
[106] Y. Kim, X. Zhao, *Chem. Rev.* **2022**, *122*, 5317.
[107] Y. Kim, H. Yuk, R. Zhao, S. A. Chester, X. Zhao, *Nature* **2018**, *558*, 274.
[108] H.-W. Huang, M. S. Sakar, A. J. Petruska, S. Pané, B. J. Nelson, *Nat. Commun.* **2016**, *7*, 12263.
[109] G. Z. Lum, Z. Ye, X. Dong, H. Marvi, O. Erin, W. Hu, M. Sitti, *Proc. Natl. Acad. Sci. U. S. A.* **2016**, *113*, E6007.
[110] H. Zhu, Y. Wang, Y. Ge, Y. Zhao, C. Jiang, *Adv. Sci.* **2022**, *9*, 2203711.
[111] W. Hu, G. Z. Lum, M. Mastrangeli, M. Sitti, *Nature* **2018**, *554*, 81.
[112] X. Du, H. Cui, T. Xu, C. Huang, Y. Wang, Q. Zhao, Y. Xu, X. Wu, *Adv. Funct. Mater.* **2020**, *30*, 1909202.
[113] Q. Ze, S. Wu, J. Nishikawa, J. Dai, Y. Sun, S. Leanza, C. Zemelka, L. S. Novelino, G. H. Paulino, R. R. Zhao, *Sci Adv.* **2022**, *8*, eabm7834.
[114] Z. Chen, Y. Lin, G. Zheng, Y. Yang, Y. Zhang, S. Zheng, J. Li, J. Li, L. Ren, L. Jiang, *ACS Appl. Mater. Interfaces* **2020**, *12*, 58179.
[115] B. Zou, Z. Liang, D. Zhong, Z. Cui, K. Xiao, S. Shao, J. Ju, *Adv. Mater.* **2023**, *35*, 2207349.
[116] Q. Ze, X. Kuang, S. Wu, J. Wong, S. M. Montgomery, R. Zhang, J. M. Kovitz, F. Yang, H. J. Qi, R. Zhao, *Adv. Mater.* **2020**, *32*, 1906657.
[117] S. Yi, L. Wang, Z. Chen, J. Wang, X. Song, P. Liu, Y. Zhang, Q. Luo, L. Peng, Z. Wu, C. F. Guo, L. Jiang, *Nat. Commun.* **2022**, *13*, 4177.
[118] H. Song, H. Lee, J. Lee, J. K. Choe, S. Lee, J. Y. Yi, S. Park, J.-W. Yoo, M. S. Kwon, J. Kim, *Nano Lett.* **2020**, *20*, 5185.
[119] A. V. Pozhitkova, D. V. Kladko, D. A. Vinnik, S. V. Taskaev, V. V. Vinogradov, *ACS. Appl. Mater. Interfaces* **2022**, *14*, 23896.
[120] A. Garcia Diez, C. Rial Tubio, J. Gutierrez Etxebarria, S. Lanceros-Mendez, *Adv. Eng. Mater.* **2021**, *23*, 2100240.
[121] E. Siéfert, N. Cattaud, E. Reyssat, B. Roman, J. Bico, *Phys. Rev. Lett.* **2021**, *127*, 168002.
[122] F. Agnelli, M. Tricarico, A. Constantinescu, *Extreme Mech. Lett.* **2021**, *42*, 101089.
[123] X. Kuang, J. Wu, K. Chen, Z. Zhao, Z. Ding, F. Hu, D. Fang, H. J. Qi, *Sci. Adv.* **2019**, *5*, eaav5790.
[124] J. Wong, A. Basu, M. Wende, N. Boechler, A. Nelson, *ACS Appl. Mater. Interfaces* **2020**, *2*, 2504.
[125] A. Basu, J. Wong, B. Cao, N. Boechler, A. J. Boydston, A. Nelson, *ACS Appl. Mater. Interfaces* **2021**, *13*, 19263.
[126] C. E. Wisinger, L. A. Maynard, J. R. Barone, *Soft Matter* **2019**, *15*, 4541.
[127] C. Yuan, T. Wang, M. L. Dunn, H. J. Qi, *Int. J. Precis. Eng. Manuf.-Green Technol.* **2017**, *4*, 281.
[128] J. M. Robertson, A. H. Torbati, E. D. Rodriguez, Y. Mao, R. M. Baker, H. J. Qi, P. T. Mather, *Soft Matter* **2015**, *11*, 5754.
[129] Y. Mao, J. M. Robertson, X. Mu, P. T. Mather, H. J. Qi, *J. Mech. Phys. Solids* **2015**, *85*, 219.
[130] O. Rabaux, R. Riva, L. Noels, C. Jerome, *Macromol. Mater. Eng.* **2022**, *307*, 2200270.
[131] J. Tang, Z. Chen, Y. Cai, J. He, Y. Luo, *Adv. Funct. Mater.* **2022**, *34*, 2203308.
[132] G. Kofod, W. Wirges, M. Paajanen, S. Bauer, *Appl. Phys. Lett.* **2007**, *90*, 081916.
[133] G. Kofod, M. Paajanen, S. Bauer, *Appl. Phys. A* **2006**, *85*, 141.
[134] S. Shian, K. Bertoldi, D. R. Clarke, *Adv. Mater.* **2015**, *27*, 6814.
[135] A. Baranwal, P. K. Agnihotri, *Compos. Sci. Technol.* **2022**, *230*, 109724.
[136] G.-K. Lau, K.-R. Heng, A. S. Ahmed, M. Shrestha, *Appl. Phys. Lett.* **2017**, *110*, 182906.
[137] G.-K. Lau, F.-Y. Chen, Z.-X. Ren, *Appl. Phys. Lett.* **2022**, *120*, 012903.
[138] J.-H. Youn, S. M. Jeong, G. Hwang, H. Kim, K. Hyeon, J. Park, K.-U. Kyung, *Appl. Sci.* **2020**, *10*, 640.
[139] B. Aksoy, H. Shea, *Adv. Funct. Mater.* **2020**, *30*, 2001597.
[140] S. Watanabe, Y. Ikemoto, J. Shintake, *Adv. Eng. Mater.* **2023**, *25*, 2201741.
[141] J. Hubertus, S. Croce, J. Neu, S. Seelecke, G. Rizzello, G. Schultes, *Adv. Funct. Mater.* **2023**, *33*, 2214176.
[142] E. Hajiesmaili, D. R. Clarke, *Nat. Commun.* **2019**, *10*, 183.
[143] T. Nagai, J. Shintake, *Polymers* **2022**, *14*, 4549.
[144] J. von Szczepanski, D. M. Opris, *Adv. Mater. Technol.* **2023**, *8*, 2201372.

[145] J. von Szczepanski, P. M. Danner, D. M. Opris, *Adv. Sci.* **2022**, *9*, 2202153.
[146] Y. Xia, G. Cedillo-Servin, R. D. Kamien, S. Yang, *Adv. Mater.* **2016**, *28*, 9637.
[147] Y. Xia, X. Zhang, S. Yang, *Angew. Chem., Int. Ed.* **2018**, *57*, 5665.
[148] A. S. Kuenstler, Y. Chen, P. Bui, H. Kim, A. DeSimone, L. Jin, R. C. Hayward, *Adv. Mater.* **2020**, *32*, 2000609.
[149] Y. Huang, H. K. Bisoyi, S. Huang, M. Wang, X.-M. Chen, Z. Liu, H. Yang, Q. Li, *Angew. Chem., Int. Ed.* **2021**, *60*, 11247.
[150] O. M. Wani, H. Zeng, A. Priimagi, *Nat. Commun.* **2017**, *8*, 15546.
[151] X. Lu, H. Zhang, G. Fei, B. Yu, X. Tong, H. Xia, Y. Zhao, *Adv. Mater.* **2018**, *30*, 1706597.
[152] Y. Liu, B. Xu, S. Sun, J. Wei, L. Wu, Y. Yu, *Adv. Mater.* **2017**, *29*, 1604792.
[153] Z. Pei, Y. Yang, Q. Chen, E. M. Terentjev, Y. Wei, Y. Ji, *Nat. Mater.* **2014**, *13*, 36.
[154] T. H. Ware, M. E. McConney, J. J. Wie, V. P. Tondiglia, T. J. White, *Science* **2015**, *347*, 982.
[155] M. Lopez-Valdeolivas, D. Liu, D. J. Broer, C. Sanchez-Somolinos, *Macromol. Rapid Commun.* **2018**, *39*, 1700710.
[156] C. P. Ambulo, J. J. Burroughs, J. M. Boothby, H. Kim, M. R. Shankar, T. H. Ware, *ACS Appl. Mater. Interfaces* **2017**, *9*, 37332.
[157] F. Feng, D. Duffy, M. Warner, J. S. Biggins, *Proc. R. Soc. A* **2022**, *478*, 20220230.
[158] M. Farhan, F. Klimm, M. Thielen, A. Resetic, A. Bastola, M. Behl, T. Speck, A. Lendlein, *Adv. Mater.* **2023**, *35*, 2211902.
[159] X. Yeli, L. Yanni, C. Yan, W. Fenjing, *Macromol. Mater. Eng.* **2022**, *307*, 2100690.
[160] Y. Liu, B. Shaw, M. D. Dickey, J. Genzer, *Sci. Adv.* **2017**, *3*, 1602417.
[161] J. Ryu, M. D'Amato, X. Cui, K. N. Long, H. J. Qi, M. L. Dunn, *Appl. Phys. Lett.* **2012**, *100*, 161908.
[162] N. Bassik, A. Brafman, A. M. Zarafshar, M. Jamal, D. Luvsanjav, F. M. Selaru, D. H. Gracias, *J. Am. Chem. Soc.* **2010**, *132*, 16314.
[163] J. Kim, S. Lee, J. Choi, K. Baek, T. S. Shim, J. Kartham Hyun, S.-J. Park, *Adv. Mater.* **2022**, *34*, 2109091.
[164] E. Siéfert, E. Reyssat, J. Bico, B. Roman, *Nat. Mater.* **2019**, *18*, 24.
[165] F. Ilievski, A. D. Mazzeo, R. F. Shepherd, X. Chen, G. M. Whitesides, *Angew. Chem., Int. Ed.* **2011**, *50*, 1890.
[166] R. F. Shepherd, F. Ilievski, W. Choi, S. A. Morin, A. A. Stokes, A. D. Mazzeo, X. Chen, M. Wang, G. M. Whitesides, *Proc. Natl. Acad. Sci. U. S. A.* **2011**, *20*, 20400.
[167] Y. Chi, Y. Tang, H. Liu, J. Yin, *Adv. Mater. Technol.* **2020**, *5*, 2000370.
[168] E. Siéfert, M. Warner, *Proc. R. Soc. A* **2020**, *476*, 2240.
[169] J. Bico, E. Siefert, B. Roman, E. Reyssat, WIPO **2021**, WO2021/224464A1.
[170] L. Belding, B. Baytekin, H. T. Baytekin, P. Rothemund, M. S. Verma, A. Nemiroski, D. Sameoto, B. A. Grzybowski, G. M. Whitesides, *Adv. Mater.* **2018**, *30*, 1704446.
[171] D. Yang, B. Mosadegh, A. Ainla, B. Lee, F. Khashai, Z. Suo, K. Bertoldi, G. M. Whitesides, *Adv. Mater.* **2015**, *27*, 6323.
[172] J. Sang, X. Li, Y. Shao, Z. Li, J. Fu, *ACS Biomater. Sci. Eng.* **2017**, *3*, 2860.
[173] M. Miotto, R. M. Gouveia, A. M. Ionescu, F. Figueiredo, I. W. Hamley, C. J. Connon, *Adv. Funct. Mater.* **2019**, *29*, 1807334.
[174] X. Zhang, Z. Meng, J. Ma, Y. Shi, H. Xu, S. Lykkemark, J. Qin, *Small* **2015**, *11*, 3666.
[175] K. Kuribayashi-Shigetomi, H. Onoe, S. Takeuchi, *PLoS One* **2012**, *7*, e51085.
[176] S. R. Shin, B. Migliori, B. Miccoli, Y.-C. Li, P. Mostafalu, J. Seo, S. Mandla, A. Enrico, S. Antona, R. Sabarish, T. Zheng, L. Pirrami, K. Zhang, Y. S. Zhang, K.-T. Wan, D. Demarchi, M. R. Dokmeci, A. Khademhosseini, *Adv. Mater.* **2018**, *30*, 1704189.
[177] M. Grosjean, C. Schmidleithner, S. Dejean, N. B. Larsen, B. Nottelet, *Mater. Des.* **2024**, *241*, 112953.
[178] A. Argiolas, B. C. Mac Murray, I. Van Meerbeek, J. Whitehead, E. Sinibaldi, B. Mazzolai, R. F. Shepherd, *Soft Rob.* **2016**, *3*, 101.

Oscar Rabaux earned a Master's degree in Advanced Materials for Innovation and Sustainability from the European Institute of Technology (EIT Raw Materials) in 2019. This program allowed him to achieve an engineering degree in Grenoble, France, and a Master of Physics from the University of Liège, Belgium. In 2023, he completed a Ph.D. in Chemical Sciences, conducting research under Professor Christine Jérôme at the Center for Education and Research on Macromolecules, supported by a FNRS–FRIA grant. His doctoral research focused on developing fully degradable polyphosphoester elastomers for use in self-folding shape memory hydrogels for biomedical applications.

Christine Jérôme is currently a Full Professor in the Chemistry Department at the University of Liege, Belgium, where she heads the Centre for Education and Research on Macromolecules (CERM). As a chemist, she has developed significant expertise in the design of polymer biomaterials. She is particularly interested in the synthesis of tailor-made biodegradable polymers and their implementation in smart, functional systems for healthcare applications. She has filed over 15 patents and is the author of more than 400 papers in international peer-reviewed journals.